Janus-type diiridium complexes with functional carbene cyclometalates for high energy phosphorescence

Guowei Ni,[a,‡] Yi Pan,[b,‡] Muyu Zhou,[a,‡] Yufeng Sang,[a] Shek-Man Yiu,[b,*] Kai Chung Lau,[b,*] Yun Chi,[a,b,*]

[‡] They contributed equally to this work.

(a) Department of Materials Science and Engineering, and Center of Super-Diamond and Advanced Films (COSDAF), City University of Hong Kong, Hong Kong SAR, E-mail: yunchi@cityu.edu.hk.

(b) Department of Chemistry, City University of Hong Kong, Hong Kong SAR, E-mail: kaichung@cityu.edu.hk and E-mail: kensmyiu@cityu.edu.hk.

Supporting Information

Experimental section:

Photophysical measurements: All photophysical measurements of this study were performed at room temperature (298 K). UV-visible spectra were recorded on a HITACHI UH4150 instrument. The emission spectra in solution were measured with an Edinburgh FLS 1000 instrument. Both wavelength-dependent excitation and emission responses were calibrated. Steady-state absorption and emission spectra of the studied complexes were measured in toluene at RT, where spectral grade solvents were employed. To specify the quantum yield in the fluid state, samples were degassed using at least three freeze-pump-thaw cycles. The solution quantum yields are calculated using coumarin 102 that has a known quantum yield, according to the following equation:

$$\Phi = \Phi_R \frac{I}{I_R} \frac{A_R}{A} \frac{\eta^2}{\eta_R^2}$$

Where Φ is the PL quantum yield, the subscript R refers to the reference compound of known quantum yield, I is the integrated fluorescence intensity, and η is the refractive index of solvent. A is the absorbance at the excitation wavelength with the measured absorbance between 0.05 – 0.1.

Electrochemistry: Cyclic voltammetry was conducted on a CHI660 Electrochemical Analyzer. All anodic and cathodic peak potential were referenced to the ferrocene redox couple (Fc/Fc^+ = 0.38 V). Oxidation and reduction potentials were measured using platinum working electrode with 0.1 M of NBu_4PF_6 as electrolyte in CH_2Cl_2. The potential was referenced externally to a ferrocene/ferrocenium (Fc/Fc^+) couple.

Single crystal X-ray diffraction: The single crystal was placed in a microfocus sealed tube and mounted on the goniometer. Diffraction data were collected on a Bruker D8 VENTURE KAPPA diffractometer using a multilayer mirror as monochromator and a Bruker PHOTON III CPAD detector. The diffractometer was equipped with an Oxford Cryostream 1000 low temperature device and Cu K_α radiation (λ = 1.54178 Å). All data were integrated with SAINT, and a multi-scan absorption correction using SADABS 2016/2 was applied. The structure was solved by Intrinsic Phasing methods with SHELXT 2014/5 program and refined by full-matrix least-squares methods against F^2 using

SHELXL-2019/2. Bruker Apex3 was used for data collection. Bruker Saint was used for computing both cell refinement and data reduction. Structure solution and refinement was computed using SHELXT-2014/5 and SHELXL-2016/6 programs, respectively. All non-hydrogen atoms were refined with anisotropic displacement parameters. All C-bound hydrogen atoms were refined isotropically on calculated positions using a riding model with their U_{iso} values constrained to 1.5 times the U_{eq} of their pivot atoms for terminal sp^3 carbon atoms and 1.2 times for all other carbon atoms. Crystallographic data were deposited with the Cambridge Crystallographic Data Centre. CCDC 2493844 - 2493847 contained the supplementary crystallographic data for this paper. These data can be obtained free of charge from Cambridge Crystallographic Data Centre via www.ccdc.cam.ac.uk/ structures. The reports and CIF data files were generated using FinalCif.

Computational details of theoretical investigations: The geometries, electronic structures, and electronic excitations were investigated at the B3LYP-D3(BJ)/def2-SVP level[1-5] using Gaussian 16 programs.[6] The solvent effect of toluene was incorporated through the polarizable continuum model (PCM).[7, 8] All corresponding ground state (S_0) and lowest triplet state (T_1) geometries were optimized based on the X-ray structural data of ***f*-Ir(L_{BM})$_2$(L_{BI})**, **Ir$_2$(Js1)(L_{BM})$_4$**, **Ir$_2$(Js2)(L_{BM})$_4$**, and **Ir$_2$(Js3)(L_{IM})$_4$**. For the TD-DFT calculation,[9, 10] a total of 20 low-lying excited states ($T_1 \sim T_{10}$ and $S_1 \sim S_{10}$) were included, utilizing the optimized S_0 structure. To achieve a clear representation of the electronic excitation at the optimized S_0 structure, natural transition orbital (NTO) analysis[11] was employed. The $S_0 \rightarrow T_1$ excitation was further analyzed using the inter-fragment charge transfer (IFCT) method with the Multiwfn software,[12] and the density calculations in the IFCT analysis were performed using the Hirshfeld method.[13] The spin-orbit coupling (SOC)-TDDFT calculations[14] were conducted using the B3LYP functional with the ZORA Hamiltonian[15, 16] (SARC-ZORA-SVP for Ir and ZORA-def2-SVP for other elements), considering the optimized S_0 and T_1 structures, in ORCA (v6.0.1) software.[17] In the SOC-TDDFT calculation in toluene with COSMO model,[18] a total of 200 low-lying excited states ($T_1 \sim T_{100}$ and $S_1 \sim S_{100}$) were included. The radiative lifetime (τ_{rad}) and radiative rate (k_r) were calculated by taking the arithmetic average and Boltzmann average (at 298 K) of the SOC substates of T_1.[14]

1,3-Bis(4-(*tert*-butyl)phenyl)-5,6-dimethyl-1H-benzo[d]imidazol-3-ium hexafluorophosphate ($L_{BM}H_2$)·PF_6

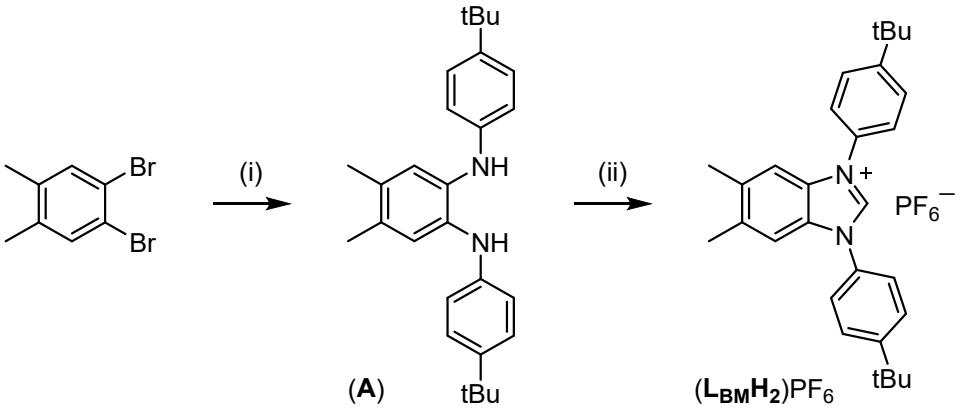

Scheme S1. Synthetic protocol to the carbene pro-chelate **($L_{BM}H_2$) PF_6**; experimental conditions: (i) 4-*tert*-butyl aniline, $Pd(OAc)_2$, 1,3-bis(2,6-diisopropylphenyl)imidazolium chloride, NaOtBu, 90°C; (ii) trimethyl orthoformate, HCl, reflux and then KPF_6.

Synthesis of N^1,N^2-bis(4-(*tert*-butyl)phenyl)-4,5-dimethylbenzene-1,2-diamine (A)

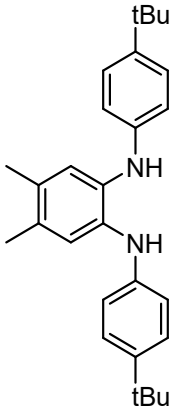

To a 50 mL flask was added $Pd(OAc)_2$ (10 mg, 0.045 mmol), 1,3-bis(2,6-diisopropylphenyl)imidazolium chloride (39 mg, 0.09 mmol), NaOtBu (0.48 g, 5.0 mmol) and degassed toluene (15 mL). The mixture was stirred for 10 minutes. After that, 1,2-dibromo-4,5-dimethylbenzene (0.6 g, 2.3 mmol) and 4-*tert*-butyl aniline (0.77 mL, 4.8 mmol) were added. The reaction mixture was then heated to 90°C for 4 hours. At removal of solvent under reduced pressure, the residue was dissolved in ethyl acetate and filtered through Celite. The solution was then washed with deionized water, dried over anhydrous Na_2SO_4, concentrated and further purified by silica gel column chromatography eluting with a mixture of hexane and ethyl acetate (20/1, v/v), giving a white

solid. Yield: 0.57 g, 63%.

Selected spectral data of **A**: ^{1}H NMR (400 MHz, $CDCl_3$) δ 7.25 (dt, *J* = 8.8 Hz, 2.0 Hz, 4H), 7.08 (s, 2H), 6.86 (dt, *J* = 8.8 Hz, 2.0 Hz, 4H), 5.46 (s, 2H), 2.19 (s, 6H), 1.30 (s, 18H).

Synthesis of carbene pro-chelate ($L_{BM}H_2$)·PF_6

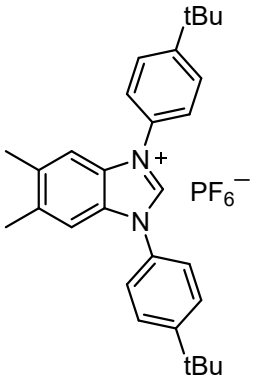

A (0.3 g, 0.75 mmol), trimethyl orthoformate (10 mL) and 1 drop of conc. HCl were added to a 50 mL flask. The reaction mixture was heated to reflux overnight. After then, the excess trimethyl orthoformate was removed under vacuum, and 5 mL of methanol was added to dissolve the residue. Then, a saturated KPF_6 solution was added to the solution dropwise with vigorous stirring to induce precipitation. The precipitation was filtered and dried under vacuum to attain a white solid of **$L_{BM}H_2$·PF_6**. Yield: 0.39 g, 94%.

Selected spectral data of **$L_{BM}H_2$·PF_6**: ^{1}H NMR (400 MHz, $CDCl_3$) δ 9.06 (s, 1H), 7.75 – 7.67 (m, 8H), 7.49 (s, 2H), 2.45 (s, 6H), 1.40 (s, 18H). ^{19}F NMR (376 MHz, $CDCl_3$): *δ* –71.67 (d, J_{PF} = 710 Hz, 6F).

1,3-Bis(3-(tert-butyl)phenyl)-1H-imidazol-3-ium triflate ($L_{IM}H_2$·OTf)

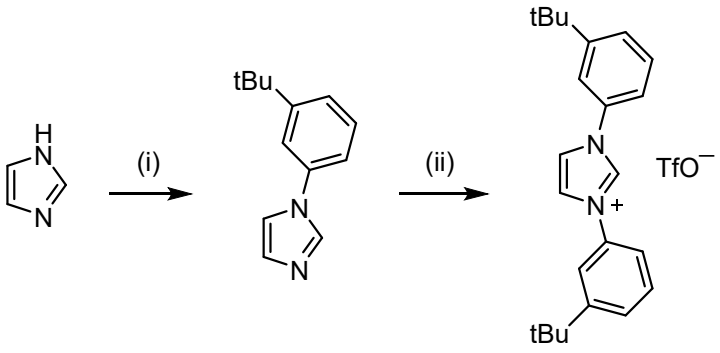

(**A2**) ($L_{IM}H_2$)OTf

Scheme S2. Synthetic protocol to the carbene pro-chelate (**$L_{IM}H_2$)·OTf**; experimental conditions: (i) 1-

bromo-3-(tert-butyl)benzene, trans-1,2-diaminocyclohexane, K_2CO_3, CuI, DMSO, 150 °C; (ii) (3-(*tert*-butyl)phenyl)(mesityl)iodonium triflate, $Cu(OAc)_2 \cdot H_2O$, DMF, 120 °C.

Synthesis of 1-(3-(tert-butyl)phenyl)-1H-imidazole (A2)

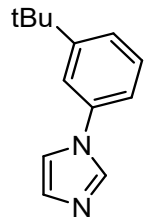

To a 100 mL flask, imidazole (0.48 g, 7.0 mmol), 1-bromo-3-(*tert*-butyl)benzene (1.15 g, 5.4 mmol), K_2CO_3 (1.5 g, 10.8 mmol), CuI (206 mg, 1.1 mmol) and trans-1,2-diaminocyclohexane (123 mg, 1.1 mmol) was suspended in 30 mL of DMSO. The suspension was then heated at 150 °C overnight under N_2 atmosphere. After cooling to RT, the mixture was diluted with 30 mL of ethyl acetate and filtered through celite. The filtrated was then poured in to 300 mL of water and extracted with 120 mL of ethyl acetate. The organic layers were combined, dried over anhydrous Na_2SO_4, concentrated and further purified via silica gel column chromatography eluting with ethyl acetate to obtain a brown oil. Yield: 0.75 g, 70%.

Selected spectral data of **A2**: ^{1}H NMR (400 MHz, $CDCl_3$) δ 7.83 (t, *J* = 1.2 Hz, 1H), 7.39 (dt, *J* = 5.2 Hz, 1.2 Hz, 2H), 7.37 – 7.34 (m, 1H), 7.27 (t, *J* = 1.2 Hz, 1H), 7.21 – 7.15 (m, 2H), 1.35 (s, 9H).

Synthesis of carbene pro-chelate ($L_{IM}H_2$)·OTf

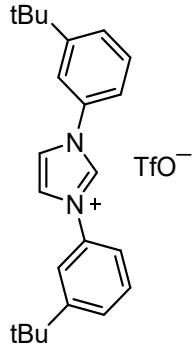

To a 50 mL flask was added **A2** (0.30 g, 1.5 mmol), (3-(*tert*-butyl)phenyl)(mesityl)iodonium triflate (0.95 g, 1.8 mmol), $Cu(OAc)_2 \cdot H_2O$ (15 mg, 0.075 mmol) and 20 mL DMF. The solution was heated at

120°C overnight. After then, the solvent was removed under reduced pressure, and the residue was dissolved in methanol. Deionized water was slowly added to the solution with vigorous stirring to induce precipitation. The precipitate was filtered and dried under vacuum to obtain a white solid. Yield: 0.67 g, 91%.

Selected spectral data of **($L_{IM}H_2$)·OTf**: ^{1}H NMR (400 MHz, $CDCl_3$) δ 9.72 (s, 1H), 7.85 (s, 2H), 7.64 (s, 2H), 7.57 (t, *J* = 8.0 Hz, 4H), 7.48 (t, *J* = 8.0 Hz, 2H), 1.36 (s, 18H). ^{19}F NMR (376 MHz, $CDCl_3$) *δ* –78.29 (s, 3F).

1-(3-(*tert*-Butyl)phenyl)-3-methyl-1H-benzo[d]imidazol-3-ium hexafluorophosphate ($L_{BI}H_2$)·PF_6

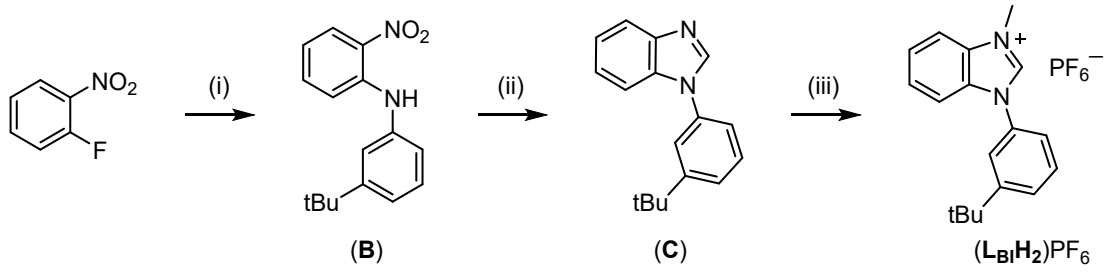

Scheme S3. Synthetic protocol to the carbene pro-chelate **($L_{BI}H_2$)·PF_6**; experimental conditions: (i) 3-*tert* butyl aniline, DMSO, 100 °C; (ii) formic acid, iron powder, reflux; (iii) MeI, acetonitrile, reflux and addition of KPF_6.

Synthesis of N-(3-(*tert*-butyl)phenyl)-2-nitroaniline (B)

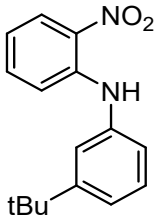

To a 50 mL flask, 2-nitrofluorobenzene (1.0 g, 7.1 mmol) and 3-*tert*-butyl aniline (2.12 g, 14.2 mmol) were dissolved in 5 mL of DMSO, and the mixture was heated to 100°C for 24 hours. After cooled to RT, 40 mL of CH_2Cl_2 was added. The mixture was washed with 30 mL of DI water three times, the organic phase was separated, dried over anhydrous Na_2SO_4 and concentrated via rotary evaporation. The crude product was further purified by flash column chromatography eluting with hexane and ethyl acetate (20/1, v/v) to attain a red oil. Yield: 1.89 g, 98%.

Selected spectral data of **B**: ^{1}H NMR (400 MHz, $CDCl_3$) δ 9.53 (s, 1H), 8.21 (dd, *J* = 8.8 Hz, 1.6 Hz, 1H), 7.39 – 7.31 (m, 2H), 7.29 – 7.24 (m, 2H), 7.21 (d, *J* = 8.8 Hz, 1H), 7.10 (d, *J* = 7.8 Hz, 1H), 6.76 (dt, *J* = 8.4 Hz, 1.2 Hz, 1H), 1.34 (s, 9H).

Synthesis of 1-(3-(*tert*-butyl)phenyl)-1H-benzo[d]imidazole (C)

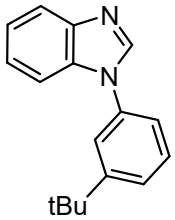

To a 100 mL flask, **B** (1.97 g, 7.29 mmol) and iron powder (2.45 g, 43.7 mmol) were dissolved in 50 mL of formic acid, and the mixture was heated to reflux for 48 hours under N_2. At end of the reaction, formic acid was evaporated under reduced pressure. The residue was dissolved in ethyl acetate and filtered through Celite. The filtrate was washed with a saturated solution of $NaHCO_3$ and dried over anhydrous Na_2SO_4. The crude product was further purified via flash column chromatography eluting with hexane and ethyl acetate (3/1, v/v) to obtain a gray solid. Yield: 1.64 g, 90%.

Selected spectral data of **C**: ^{1}H NMR (400 MHz, $CDCl_3$) δ 8.14 (s, 1H), 7.93 – 7.85 (m, 1H), 7.58 – 7.45 (m, 4H), 7.39 – 7.28 (m, 3H), 1.39 (s, 9H).

Synthesis of carbene pro-chelate ($L_{BI}H_2$)·PF_6

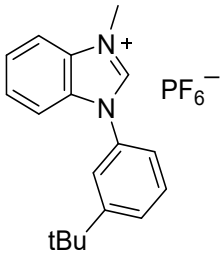

To a 38 mL seal tube, **C** (1 g, 4.0 mmol) and methyl iodide (0.28 mL, 4.4 mmol) were dissolved in 15 mL of acetonitrile. The mixture was heated to reflux overnight under N_2. Next, the solvent was evaporated under reduced pressure and the residue was dissolved in 5 mL of methanol. Saturated KPF_6 solution in water was added dropwise with vigorous stirring to induce precipitation. The

precipitate was filtered and then dried under vacuum to obtain a white solid of $\mathbf{L_{BI}H_2{\cdot}PF_6}$. Yield: 1.28 g, 78%.

Selected spectral data of $\mathbf{(L_{BI}H_2){\cdot}PF_6}$: ^{1}H NMR (400 MHz, $CDCl_3$) δ 9.27 (s, 1H), 7.83 (d, *J* = 8.4 Hz, 1H), 7.76 – 7.62 (m, 5H), 7.57 (dt, *J* = 8.4 Hz, 1.6 Hz, 1H), 7.45 (dt, *J* = 8.4 Hz, 1.6 Hz, 1H), 4.24 (s, 3H), 1.38 (s, 9H). ^{19}F NMR (376 MHz, $CDCl_3$): δ –71.67 (d, J_{PF} = 710 Hz, 6F).

Janus carbene pro-chelates $(Js1H_4){\cdot}2PF_6$ and $(Js2H_4){\cdot}2PF_6$

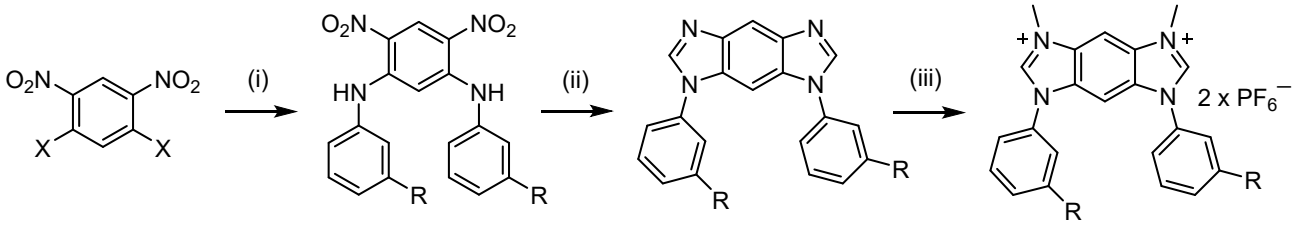

X = Cl or F

R = H, (**D1**)
R = tBu, (**D2**)

R = H, (**E1**)
R = tBu, (**E2**)

R = H, (**Js1**H_4)$(PF_6)_2$
R = tBu, (**Js2**H_4)$(PF_6)_2$

Scheme S4. Synthetic protocol to the Janus carbene pro-chelates; experimental conditions: (i) aniline, Et_3N, iPrOH, reflux; (ii) formic acid, iron powder, reflux; (iii) MeOTf, acetonitrile, reflux and then KPF_6.

Synthesis of 4,6-dinitro-N^1,N^3-diphenylbenzene-1,3-diamine (D1)

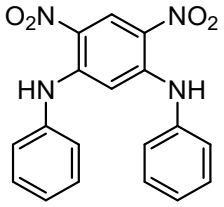

1,5-Dichloro-2,4-dinitrobenzene (0.25 g, 1.05 mmol), aniline (0.39 mL, 4.2 mmol), and triethyl amine (0.45 mL, 3.15 mmol) were dissolved in 20 mL of isopropanol, and the solution was heated to reflux overnight. After cooled to RT, the precipitates were filtered and washed with DI water and isopropanol in sequence for three times. The resulting residue was dried under vacuum without further purification. Yield: 0.35 g, 95%.

Selected spectral data of **D1**: ^{1}H NMR (400 MHz, $CDCl_3$) δ 9.75 (s, 2H), 9.34 (s, 1H), 7.34 (tt, *J* = 7.6 Hz, 2.0 Hz, 4H), 7.20 (tt, *J* = 7.6 Hz, 1.6 Hz, 2H), 7.15 (d, *J* = 7.2 Hz, 4H), 6.53 (s, 1H).

Synthesis of N^1,N^3-bis(3-(*tert*-butyl)phenyl)-4,6-dinitrobenzene-1,3-diamine (D2)

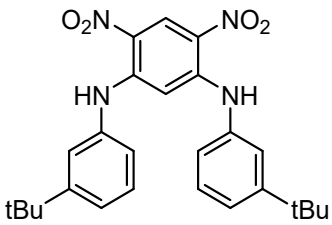

The procedure was analogous to that described for **D1** and it was obtained from 3-*tert*-butyl aniline (1 mL, 6.3 mmol) as a yellow solid. Yield: 0.74 g, 76%.

Selected spectral data of **D2**: ^{1}H NMR (400 MHz, $CDCl_3$) δ 9.78 (s, 2H), 9.35 (s, 1H), 7.25 – 7.16 (m, 4H), 7.09 (t, *J* = 1.6 Hz, 2H), 6.94 (dt, *J* = 7.6 Hz, 1.6 Hz, 2H), 6.66 (s, 1H), 1.16 (s, 18H).

Synthesis of 1,7-diphenyl-1,7-dihydrobenzo[1,2-d:4,5-d']diimidazole (E1)

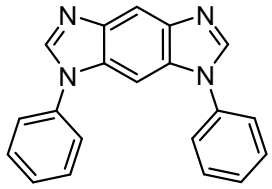

D1 (0.3 g, 0.86 mmol) and iron powder (580 mg, 10.3 mmol) were suspended in 20 mL of formic acid, and the mixture was heated to reflux for 36 hours under N_2. At end of the reaction, formic acid was evaporated under reduced pressure. The residue was dissolved in ethyl acetate, and filtered through celite. The filtrate was neutralized with a saturated solution of $NaHCO_3$ and dried over anhydrous Na_2SO_4. The crude product was further purified via silica gel column chromatography with hexane/ethyl acetate (1/1, v/v) as eluent to afford a gray solid. Yield: 0.23 g, 85%.

Selected spectral data of **E1**: ^{1}H NMR (400 MHz, $CDCl_3$) δ 8.34 (s, 1H), 8.16 (s, 2H), 7.61 – 7.55 (m, 5H), 7.53 (dt, *J* = 7.2 Hz, 1.6 Hz, 4H), 7.46 (tt, *J* = 7.2 Hz, 1.6 Hz, 2H).

Synthesis of 1,7-bis(3-(*tert*-butyl)phenyl)-1,7-dihydrobenzo[1,2-d:4,5-d']diimidazole (E2)

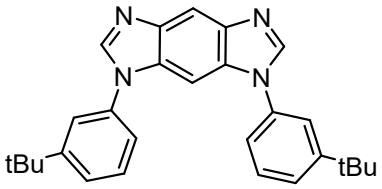

The procedure was analogous to that described for **E1**. **E2** was obtained from **D2** (0.5 g, 1.08 mmol) as a gray solid. Yield: 0.43 g, 95%.

Selected spectral data of **E2**: ^{1}H NMR (400 MHz, $CDCl_3$) δ 8.34 (s, 1H), 8.18 (s, 2H), 7.58 (s, 1H), 7.53 (s, 2H), 7.50 – 7.45 (m, 4H), 7.39 – 7.32 (m, 2H), 1.36 (s, 18H).

Synthesis of Janus dicarbene pro-chelate (Js1H$_4$)·2PF$_6$

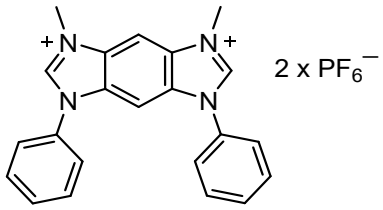

In a 50 mL round bottom flask, **E1** (140 mg, 0.45 mmol) and methyl trifluoromethanesulfonate (155 mg, 0.95 mmol) were dissolved in acetonitrile (10 mL) and the mixture was heated to reflux overnight. Next, the solvent was evaporated under reduced pressure and the residue was dissolved in 10 mL of methanol. Saturated KPF_6 solution in water was added dropwise with vigorous stirring to induce precipitation. The precipitate was filtered and then dried under vacuum to obtain a white solid of **(Js1H$_4$)·2PF$_6$**. Yield: 198 mg, 70%.

Selected spectral data of **(Js1H$_4$)·2PF$_6$**: ^{1}H NMR (400 MHz, DMSO-d_6) δ 10.39 (s, 2H), 9.07 (s, 1H), 8.07 (s, 1H), 7.87 (dt, *J* = 6.8 Hz, 1.6 Hz, 4H), 7.78 – 7.68 (m, 6H), 4.28 (s, 6H). ^{19}F NMR (376 MHz, DMSO-d_6) δ –69.23 (d, J_{PF} = 710 Hz, 12F).

Synthesis of Janus dicarbene pro-chelate (Js2H$_4$)·2PF$_6$

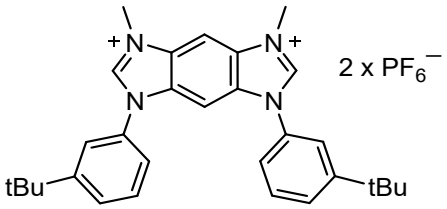

The procedure was analogous to that described for **(Js1H$_4$)·2PF$_6$**. The respective **(Js2H$_4$)·2PF$_6$** was obtained from **E2** (0.31 g, 0.73 mmol) as a white solid. Yield: 0.43 g, 78%.

Selected spectral data of **(Js2H$_4$)·2PF$_6$**: ^{1}H NMR (400 MHz, DMSO-d_6) δ 10.40 (s, 2H), 9.09 (s, 1H), 7.98 (s, 1H), 7.87 (t, *J* = 2.0 Hz, 2H), 7.73 (d, *J* = 8.0 Hz, 4H), 7.65 (t, *J* = 8.0 Hz, 2H), 4.29 (s, 6H), 1.34 (s, 18H). ^{19}F NMR (376 MHz, DMSO-d_6) δ –69.22 (d, J_{PF} = 710 Hz, 12F).

Janus carbene pro-chelate (JS3)

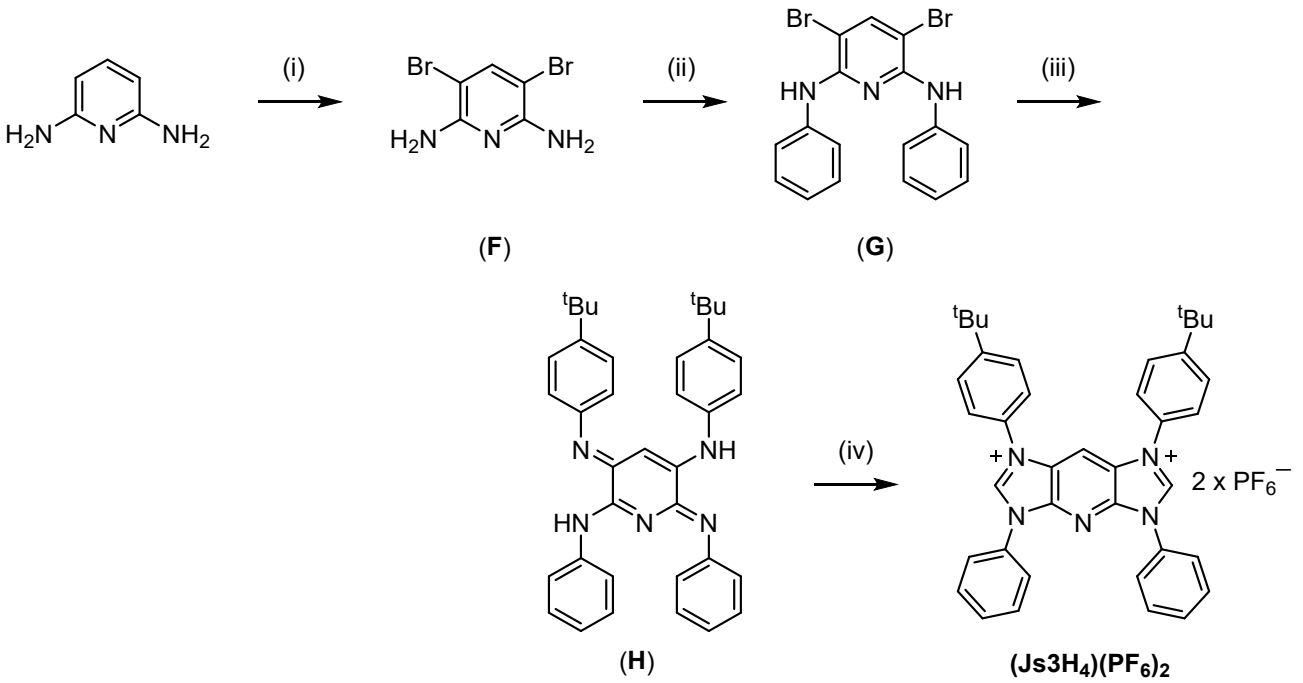

Scheme S5. Synthetic protocol to the Janus carbene pro-chelate **(Js3H$_4$)·2PF$_6$**; experimental conditions: (i) NBS, CH_2Cl_2, 0°C; (ii) iodobenzene, $Pd(OAc)_2$, Xantphos, Cs_2CO_3, tert-butanol, reflux; (iii) 4-tert-butyl aniline, Brettphos-Pd-G3, LiHMDS, toluene, reflux; (iv) paraformaldehyde, HCl, toluene, reflux; then paraformaldehyde, HCl, toluene, $Pd(OAc)_2$ and ^{i}PrOH, 50°C and then KPF_6.

Synthesis of 2,6-diamino-3,5-dibromopyridine (F)

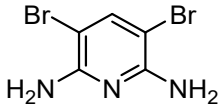

To a 100 mL flask, 2,6-diaminopyridine (1.0 g, 9.2 mmol) was dissolved in 40 mL of CH_2Cl_2. Then, NBS (3.4 g, 19.3 mmol) was added to the mixture portion wise at 0 °C stirred for 20 minutes. At the end of the reaction, the precipitate was filtered and dissolved in ethyl acetate, sequentially washed with saturated solution of sodium thiosulfate ($Na_2S_2O_3$) and deionized water, dried over anhydrous Na_2SO_4 and then concentrated to dryness under reduced pressure to afford an off-white solid without further purification. Yield: 1.3 g, 55%.

Selected spectral data of **F**: ^{1}H NMR (400 MHz, DMSO-d_6) δ 8.55 (s, 1H), 5.86 (s, 4H).

Synthesis of 3,5-dibromo-N^2,N^6-diphenylpyridine-2,6-diamine (G)

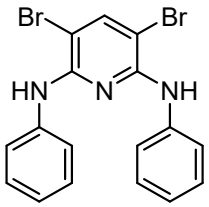

To a 50 mL flask was added **F** (0.25 g, 0.94 mmol), iodobenzene (0.40 g, 2.0 mmol), $Pd(OAc)_2$ (21 mg, 0.094 mmol), Xantphos (54 mg, 0.094 mmol), Cs_2CO_3 (0.86 g, 2.6 mmol) and *tert*-butanol (20 mL). The reaction mixture was then refluxed overnight under N_2 atmosphere. At the end of the reaction, the solvent was removed under reduced pressure. The residue was dissolved in ethyl acetate and filtered through Celite. The filtrate was washed with a saturated solution of $NaHCO_3$ and deionized water, dried over anhydrous Na_2SO_4 and further purified via silica gel column chromatography eluting with hexane and CH_2Cl_2 (10/1, v/v) to obtain a white solid. Yield: 0.18 g, 46%.

Selected spectral data of **G**: ^{1}H NMR (400 MHz, $CDCl_3$) δ 7.73 (s, 1H), 7.47 (d, *J* = 7.6 Hz, 4H), 7.27 (t, *J* = 7.6 Hz, 4H), 7.06 (t, *J* = 7.6 Hz, 2H), 6.86 (s, 2H).

Synthesis of (3E,6Z)-N^5-(4-(tert-butyl)phenyl)-3-((4-(tert-butyl)phenyl)imino)-N^2-phenyl-6-(phenylimino)-3,6-dihydropyridine-2,5-diamine (H)

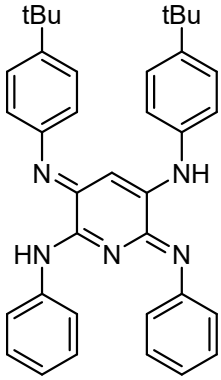

To a 50 mL flask was added **G** (0.50 g, 1.20 mmol), 4-*tert*-butyl aniline (0.54 g, 3.6 mmol), Brettphos-Pd-G3 (55 mg, 0.06 mmol), LiHMDS (9.6 mL, 9.6 mmol, 1 M in toluene) and toluene (10 mL). The reaction mixture was then refluxed overnight under N_2 atmosphere. At the end of the reaction, the solvent was removed under reduced pressure. The residue was dissolved in ethyl acetate then filtered through Celite, washed with deionized water, dried over anhydrous Na_2SO_4, and further purified by silica gel column chromatography eluting with a mixture of hexane and ethyl acetate (20/1, v/v), giving a red solid. Yield: 0.32 g, 48%.

Selected spectral data of **H**: ^{1}H NMR (400 MHz, $CDCl_3$) δ 8.83 (s, 2H), 7.55 (d, *J* = 7.6 Hz, 4H), 7.36 (d, *J* = 8.4 Hz, 4H), 7.31 (t, *J* = 7.6 Hz, 4H), 7.12 (t, *J* = 7.6 Hz, 2H), 7.01 (d, *J* = 8.4 Hz, 4H), 6.34 (s, 1H), 1.31 (s, 18H).

Synthesis of Janus dicarbene pro-chelate (Js3H$_4$)·2PF$_6$

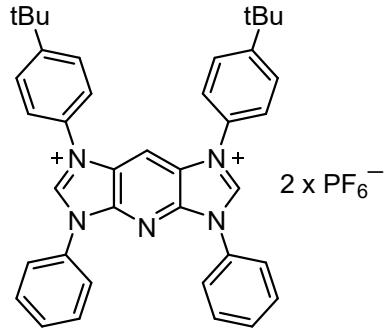

To a 50 mL flask was added **H** (100 mg, 0.18 mmol), paraformaldehyde (54 mg, 1.8 mmol) and 10 mL of toluene. A drop of concentrated HCl was added as catalyst. The solution was refluxed for 4 hours to afford a greenish-yellow precipitation, which was filtered and washed with hexane.

This as-prepared intermediate, paraformaldehyde (54 mg, 1.8 mmol), and $Pd(OAc)_2$ (1 mg, 0.004 mmol) were suspended a mixed solvent of toluene and isopropanol (10 mL, v/v = 10/1). After the addition of a drop of concentrated $HCl_{(aq)}$, the suspension was stirred at 50°C overnight. At the end of the reaction, the solvent was removed under reduced pressure, and the residue was dissolved in 10 mL of methanol. Saturated KPF_6 aqueous solution was added dropwise with vigorous stirring to induce precipitation. The precipitate was filtered and then dried under vacuum to obtain a brown solid of **(Js3H$_4$)·2PF$_6$**. Yield: 102 mg, 65%.

Selected spectral data of **(Js3H$_4$)·2PF$_6$**: ^{1}H NMR (400 MHz, DMSO-d_6) δ 11.09 (s, 2H), 9.20 (s, 1H), 8.03 (d, *J* = 8.8 Hz, 4H), 7.35 – 7.28 (m, 8H), 7.10 (d, *J* = 8.8 Hz, 4H), 7.03 (t, *J* = 7.2 Hz, 2H), 1.40 (s, 18H). ^{19}F NMR (376 MHz, DMSO-d_6) δ –69.20 (d, J_{PF} = 710 Hz, 12F).

General procedure for synthesis of mono- and dinuclear Ir(III) complexes

To a 50 mL flask was added **(L$_{BM}$H$_2$)·PF$_6$** (148 mg, 0.296 mmol), $[Ir(COD)(\mu\text{-}Cl)]_2$ (50 mg, 0.074 mmol), NaOAc (61 mg, 0.74 mmol) and anhydrous acetonitrile (15 mL). The mixture was first refluxed for 8 hours, and solvent was stripped to dryness. To the residue was added the second or Janus

carbene pro-chelate (0.074 mmol), NaOAc (61 mg, 0.74 mmol) and 1,2-dichlorobenzene (15 mL). The mixture was next refluxed overnight under N_2. After cooling to RT, the solvent was removed, and residue was purified using silica gel column chromatography eluting with a mixture of hexane and ethyl acetate (6/1, v/v) to afford the anticipated dinuclear Ir(III) complex, together with modest amount of homoleptic ***f*-Ir(L_{BM})$_3$** as co-product.

Synthesis of *f*-Ir(L_{BM})$_2$(L_{BI})

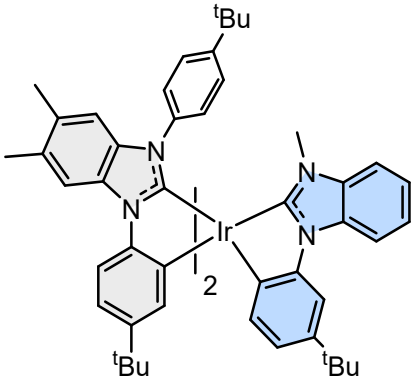

***f*-Ir(L_{BM})$_2$(L_{BI})**

The procedure was analogous to that described in the general procedure. The desired colorless product ***f*-Ir(L_{BM})$_2$(L_{BI})** (85 mg, 45%) was obtained from **($L_{BM}H_2$)·PF_6** (148 mg, 0.296 mmol) and **($L_{BI}H_2$)·PF_6** (67 mg, 0.163 mmol).

Selected spectral data of ***f*-Ir(L_{BM})$_2$(L_{BI})**: HRMS (ESI) for $C_{76}H_{85}IrN_6$ $[M + 1]^+$: calcd 1275.6499, found 1275.6599; ^{1}H NMR (400 MHz, CD_2Cl_2) δ 8.05 (d, *J* = 8.4 Hz, 1H), 8.03 (s, 1H), 7.92 (d, *J* = 8.4 Hz, 1H), 7.90 (s, 1H), 7.86 (d, *J* = 2.0 Hz, 1H), 7.70 (d, *J* = 8.0 Hz, 1H), 7.59 (dd, *J* = 8.4 Hz, 2.4 Hz, 1H), 7.35 (dd, *J* = 8.4 Hz, 2.4 Hz, 1H), 7.23 (t, *J* = 7.2 Hz, 1H), 7.16 – 7.06 (m, 3H), 6.94 (dd, *J* = 8.4 Hz, 2.4 Hz, 1H), 6.82 (d, *J* = 8.0 Hz, 1H), 6.76 (dd, *J* = 8.0 Hz, 1.6 Hz, 1H), 6.75 (s, 1H), 6.60 (d, *J* = 2.4 Hz, 1H), 6.47 - 6.31 (m, 4H), 6.17 (s, 1H), 6.03 – 5.93 (m, 3H), 2.67 (s, 3H), 2.47 (s, 3H), 2.39 (s, 3H), 2.22 (s, 3H), 2.15 (s, 3H), 1.37 (s, 9H), 1.06 (s, 9H), 1.04 (s, 9H), 0.96 (s, 18H).

Selected crystal data of ***f*-Ir(L_{BM})$_2$(L_{BI})**: CCDC number: 2493846. $C_{77}H_{87}Cl_2IrN_6$; M = 1359.62; monoclinic; space group 14: $P2_1/c$; *a* = 13.1678(4) Å, *b* = 45.4005(13) Å, *c* = 11.9060(3) Å; β = 107.720(2)°; V = 6780.0(3) Å^3; Z = 4; ρ_{Calcd} = 1.332 g·cm^{-3}; μ = 4.891 mm^{-1}; F(000) = 2808, λ(Cu-K$_\alpha$) = 1.54178 Å; T = 213 (2) K; crystal size / mm^3: 0.03 × 0.17 × 0.28; 50789 reflections collected, 13747

independent reflections (R_{int} = 0.0844), data / restraints / parameters = 13747/108/822, GOF = 1.045, final $R_1[I > 2\sigma(I)]$ = 0.0488 and wR_2(all data) = 0.1338.

Synthesis of $Ir_2(Js1)(L_{BM})_4$

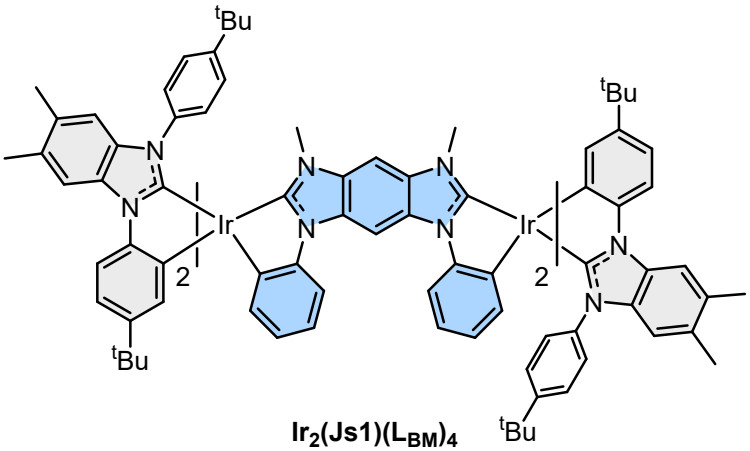

$Ir_2(Js1)(L_{BM})_4$

The procedure was analogous to that described in the general procedure. The desired dinuclear complex **$Ir_2(Js1)(L_{BM})_4$** was obtained as a white solid (42 mg, 24%) from **$(L_{BM}H_2)\cdot PF_6$** (148 mg, 0.296 mmol) and **$(Js1H_4)\cdot 2PF_6$** (47 mg, 0.074 mmol) along with homoleptic Ir(III) complex ***f*-$Ir(L_{BM})_3$** (35 mg, 17%).

Selected spectral data of **$Ir_2(Js1)(L_{BM})_4$**: HRMS (ESI) for $C_{138}H_{148}Ir_2N_{12}$ $[M + 1]^+$: calcd 2360.1242, found 2360.1435; ^{1}H NMR (400 MHz, CD_2Cl_2) δ 8.63 (s, 1H), 8.00 (d, *J* = 4.6 Hz, 4H), 7.92 (t, *J* = 8.0 Hz, 4H), 7.74 (d, *J* = 8.0 Hz, 2H), 7.52 (dd, *J* = 8.4 Hz, 2.4 Hz, 2H), 7.33 (dd, *J* = 8.4 Hz, 2.4 Hz, 2H), 7.14 (t, *J* = 7.2 Hz, 2H), 7.10 (dd, *J* = 8.4 Hz, 2.4 Hz, 2H), 6.95 (dd, *J* = 8.4 Hz, 2.4 Hz, 2H), 6.87 (d, *J* = 8.0 Hz, 2H), 6.81 (d, *J* = 2.4 Hz, 2H), 6.75 (s, 2H), 6.71 (t, *J* = 7.6 Hz, 2H), 6.58 (dd, *J* = 6.0 Hz, 1.6 Hz, 2H), 6.56 (s, 2H), 6.49 (dd, *J* = 8.4 Hz, 2.4 Hz, 2H), 6.36 (dd, *J* = 8.4 Hz, 2.0 Hz, 2H), 6.05 (s, 2H), 5.99 (s, 1H), 5.97 (dd, *J* = 8.0 Hz, 2.0 Hz, 2H), 5.93 – 5.84 (m, 4H), 2.69 (s, 6H), 2.45 (s, 6H), 2.44 (s, 6H), 2.23 (s, 6H), 2.11 (s, 6H), 1.06 (s, 18H), 0.99 (s, 36H), 0.17 (s, 18H).

Selected crystal data of **$Ir_2(Js1)(L_{BM})_4$**: CCDC number: 2493844. $C_{144}H_{160}Cl_{12}Ir_2N_{12}$; M = 2868.63; monoclinic; space group 15: C2/c; *a* = 24.7568(17) Å, *b* = 23.5695(18) Å, *c* = 28.5975(19) Å; β = 108.311(2)°; V = 15841.9(19) Å^3; Z = 4; ρ_{Calcd} = 1.203 g·cm^{-3}; μ = 5.424 mm^{-1}; F(000) = 5864, λ(Cu-K_α) = 1.54178 Å; T = 253(2) K; crystal size / mm^3: 0.04 × 0.14 × 0.29; 131736 reflections collected, 16248 independent reflections (R_{int} = 0.0574), data / restraints / parameters = 16248/2335/1114, GOF =

1.059, final $R_1[I > 2\sigma(I)]$ = 0.0318 and wR_2(all data) = 0.0902.

Selected spectral data of ***f*-Ir(L$_{BM}$)$_3$**: HRMS (ESI) for $C_{87}H_{99}IrN_6$ $[M + 1]^+$: calcd 1421.7594, found 1421.7710; ^{1}H NMR (400 MHz, $CDCl_3$) δ 7.93 (s, 3H), 7.80 (d, *J* = 8.4 Hz, 3H), 7.25 (dd, *J* = 8.4 Hz, 2.4 Hz, 3H), 7.03 (dd, *J* = 8.4 Hz, 2.4 Hz, 3H), 6.55 (d, *J* = 2.0 Hz, 3H), 6.25 (dd, *J* = 8.4 Hz, 2.4 Hz, 3H), 6.11 (dd, *J* = 8.4 Hz, 2.0 Hz, 3H), 6.10 (s, 3H), 6.04 (dd, *J* = 8.4 Hz, 2.4 Hz, 3H), 2.41 (s, 9H), 2.13 (s, 9H), 1.05 (s, 27H), 1.02 (s, 27H).

Synthesis of Ir$_2$(Js2)(L$_{BM}$)$_4$

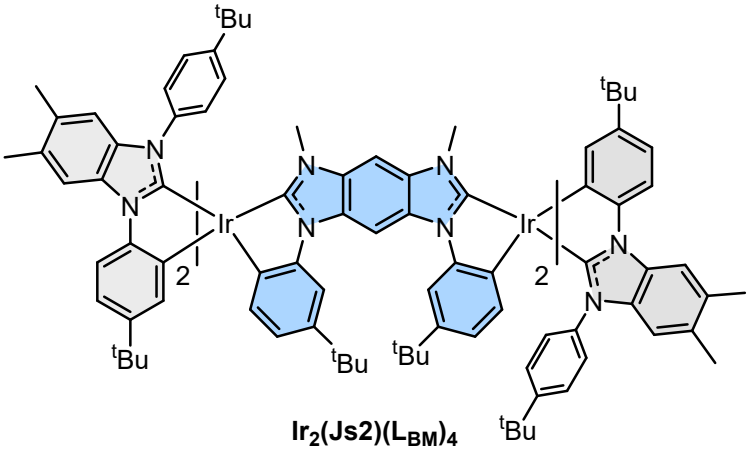

Ir$_2$(Js2)(L$_{BM}$)$_4$

The procedure was analogous to that described in the general procedure. The desired product **Ir$_2$(Js2)(L$_{BM}$)$_4$** was obtained as a white solid (51 mg, 28%) from **(L$_{BM}$H$_2$)·PF$_6$** (148 mg, 0.296 mmol) and **(Js2H$_4$)·2PF$_6$** (56 mg, 0.074 mmol) along with homoleptic Ir(III) complex ***f*-Ir(L$_{BM}$)$_3$** (32 mg, 15%).

Selected spectral data of **Ir$_2$(Js2)(L$_{BM}$)$_4$**: HRMS (ESI) for $C_{146}H_{164}Ir_2N_{12}$ $[M + 1]^+$: calcd 2472.2494, found 2472.2718; ^{1}H NMR (400 MHz, CD_2Cl_2) δ 8.50 (s, 1H), 8.00 (d, *J* = 9.6 Hz, 4H), 7.90 (d, *J* = 8.0 Hz, 2H), 7.88 (d, *J* = 2.0 Hz, 2H), 7.71 (d, *J* = 8.4 Hz, 2H), 7.51 (dd, *J* = 8.4 Hz, 2.0 Hz, 2H), 7.31 (dd, *J* = 8.4 Hz, 2.4 Hz, 2H), 7.10 (dd, *J* = 8.0 Hz, 2.4 Hz, 2H), 6.92 (dd, *J* = 8.4 Hz, 2.4 Hz, 2H), 6.89 (dd, *J* = 8.0 Hz, 1.6 Hz, 2H), 6.79 (d, *J* = 2.4 Hz, 2H), 6.77 (dd, *J* = 8.0 Hz, 1.6 Hz, 2H), 6.73 (s, 2H), 6.48 (dd, *J* = 8.4 Hz, 2.4 Hz, 2H), 6.46 (d, *J* = 7.6 Hz, 2H), 6.36 (dd, *J* = 8.4 Hz, 2.0 Hz, 2H), 6.35 (d, *J* = 2.4 Hz, 2H), 6.08 (s, 2H), 5.98 (s, 1H), 5.97 (t, *J* = 9.6 Hz, 4H), 5.83 (dd, *J* = 8.4 Hz, 2.0 Hz, 2H), 2.64 (s, 6H), 2.45 (s, 6H), 2.43 (s, 6H), 2.23 (s, 6H), 2.12 (s, 6H), 1.44 (s, 18H), 1.06 (s, 18H), 1.00 (s, 18H), 0.97 (s, 18H), 0.21 (s, 18H).

Selected crystal data of **Ir$_2$(Js2)(L$_{BM}$)$_4$**: CCDC number: 2493845. $C_{150}H_{172}Cl_8Ir_2N_{12}$; M = 2810.99; monoclinic; space group 13: P2/n; *a* = 33.7477(18) Å, *b* = 12.4772(7) Å, *c* = 33.9723(18) Å; β =

95.452(3)°; V = 14240.2(13) Å^3; Z = 4; ρ_{Calcd} = 1.311 g·cm^{-3}; μ = 5.348 mm^{-1}; F(000) = 5784, λ(Cu-K$_\alpha$) = 1.54178 Å; T = 213 (2) K; crystal size / mm^3: 0.02 × 0.03 × 0.35; 105777 reflections collected, 28872 independent reflections (R_{int} = 0.1205), data / restraints / parameters = 28872/1160/1786, GOF = 1.070, final $R_1[I > 2\sigma(I)]$ = 0.0692 and wR_2(all data) = 0.1951.

Synthesis of $Ir_2(Js3)(L_{BM})_4$

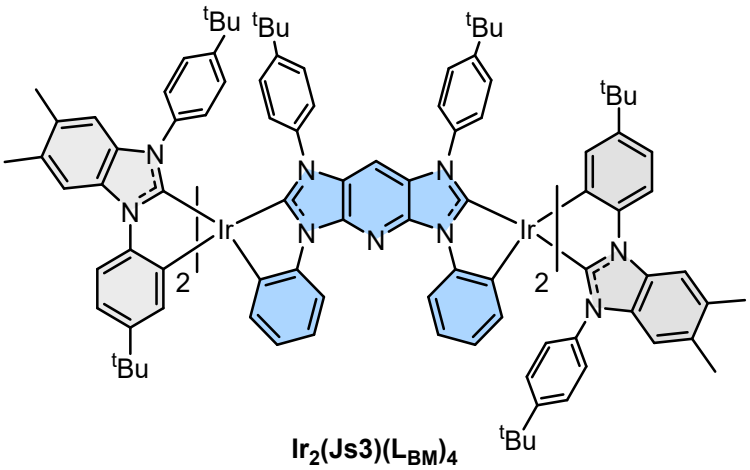

$Ir_2(Js3)(L_{BM})_4$

The procedure was analogous to that described in the general procedure. The desired dinuclear complex **$Ir_2(Js3)(L_{BM})_4$** was obtained as a yellow solid (31 mg, 16%) from **$(L_{BM}H_2)\cdot PF_6$** (148 mg, 0.296 mmol) and **$(Js3H_4)\cdot 2PF_6$** (64 mg, 0.074 mmol) along with a white solid of homoleptic Ir(III) complex ***f*-$Ir(L_{BM})_3$** (30 mg, 14%).

Selected spectral data of **$Ir_2(Js3)(L_{BM})_4$**: HRMS (ESI) for $C_{155}H_{167}Ir_2N_{13}$ $[M + 1]^+$: calcd 2597.2759, found 2597.3023; ^{1}H NMR (400 MHz, CD_2Cl_2) δ 9.18 (d, *J* = 8.0 Hz, 2H), 8.00 (s, 2H), 7.94 (s, 2H), 7.89 (d, *J* = 8.4 Hz, 2H), 7.81 (d, *J* = 8.0 Hz, 2H), 7.26 (t, *J* = 8.0 Hz, 2H), 7.22 (d, *J* = 8.4 Hz, 2H), 7.11 (dd, *J* = 8.4 Hz, 2.4Hz, 2H), 7.08 – 7.00 (m, 6H), 6.82 (d, *J* = 2.4 Hz, 2H), 6.78 (t, *J* = 7.2 Hz, 2H), 6.63 (d, *J* = 2.4 Hz, 2H), 6.59 (d, *J* = 7.2 Hz, 2H), 6.22 (dd, *J* = 8.0 Hz, 2.4 Hz, 2H), 6.19 (dd, *J* = 8.0 Hz, 2.4 Hz, 2H), 6.16 – 6.09 (m, 8H), 6.04 (s, 2H), 5.95 (dt, *J* = 8.0 Hz, 2.4 Hz, 6H), 5.87 (dd, *J* = 8.4 Hz, 2.4 Hz, 2H), 5.36 (s, 1H), 2.44 (s, 6H), 2.42 (s, 6H), 2.11 (s, 6H), 2.09 (s, 6H), 1.08 (s, 18H), 1.04 (s, 18H), 0.95 (s, 18H), 0.90 (s, 18H), 0.30 (s, 18H).

Synthesis of $Ir_2(Js3)(L_{IM})_4$

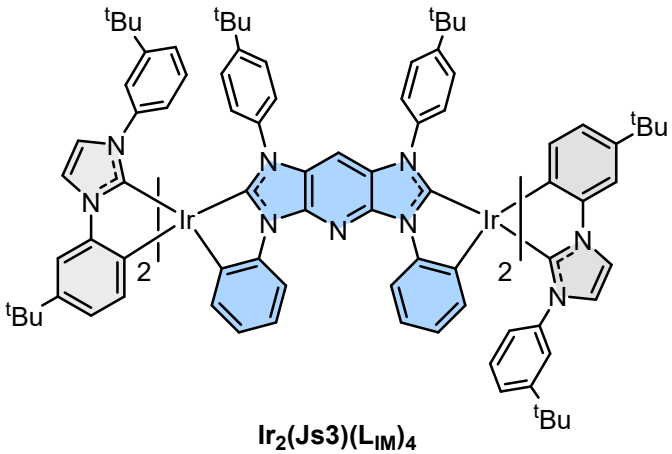

Ir_2(Js3)(L_{IM})$_4$

The procedure was analogous to that described in the general procedure. The desired dinuclear complex **Ir_2(Js3)(L_{IM})$_4$** was obtained as a yellow solid (20 mg, 12%) from **($L_{IM}H_2$)·OTf** (143 mg, 0.296 mmol) and **(Js3H_4)·2PF_6** (64 mg, 0.074 mmol) along with homoleptic Ir(III) complex ***f*-Ir(L_{IM})$_3$** (22 mg, 13%).

Selected spectral data of **Ir_2(Js3)(L_{IM})$_4$**: HRMS (ESI) for $C_{131}H_{143}Ir_2N_{13}$ $[M + 1]^+$: calcd 2285.0881, found 2285.1068; ^{1}H NMR (400 MHz, CD_2Cl_2) δ 8.87 (d, *J* = 8.0 Hz, 2H), 7.41 (d, *J* = 1.2 Hz, 2H), 7.34 – 7.25 (m, 4H), 7.22 (d, *J* =1.2 Hz, 2H), 7.19 – 7.09 (m, 6H), 7.00 (d, *J* = 8.4 Hz, 2H), 6.92 (t, *J* = 7.6 Hz, 2H), 6.75 (d, *J* = 7.6 Hz, 4H), 6.73 – 6.66 (m, 4H), 6.62 (s, 2H), 6.58 (d, *J* = 8.4 Hz, 2H), 6.53 (d, *J* = 7.6 Hz, 2H), 6.48 (d, *J* = 4.8 Hz, 2H), 6.46 (s, 2H), 6.43 (d, *J* = 1.2 Hz, 2H), 6.38 (d, *J* = 7.6 Hz, 2H), 6.33 (d, *J* = 8.0 Hz, 2H), 6.25 (t, *J* = 8.0 Hz, 2H), 6.10 (d, *J* = 8.4 Hz, 2H), 6.00 (s, 1H), 5.90 (d, *J* = 7.6 Hz, 2H), 5.78 (d, *J* = 7.6 Hz, 2H), 1.37 (s, 18H), 1.33 (s, 18H), 1.27 (s, 18H), 1.26 (s, 18H), 0.96 (s, 18H).

Selected crystal data of **Ir_2(Js3)(L_{IM})$_4$**: CCDC number: 2493847. $C_{131.50}H_{144}ClIr_2N_{13}$; M = 2326.44; orthorhombic; space group 37: Ccc2; *a* = 39.8974(9) Å, *b* = 14.5469(3) Å, *c* = 22.9823(5) Å; V = 13338.5(5) Å^3; Z = 4; ρ_{Calcd} = 1.158 g·cm^{-3}; μ = 4.354 mm^{-1}; F(000) = 4780, λ(Cu-K$_\alpha$) = 1.54178 Å; T = 193 (2) K; crystal size / mm^3: 0.02 × 0.09 × 0.28; 109555 reflections collected, 13498 independent reflections (R_{int} = 0.0541), data / restraints / parameters = 13498/1634/1038, GOF = 1.087, final R_1[$I > 2\sigma(I)$] = 0.0260 and wR_2(all data) = 0.0661.

Table S1. Electrochemical data of the studied Ir(III) complexes.

	$E^{ox}_{½}$ (V) [a] [ΔE_p]	onset λ (nm)	E_{HOMO} (eV)	E_g [b] (eV)	E_{LUMO} [b] (eV)
***f*-Ir(L_{BM})$_3$**	0.22	379	–5.02	3.27	–1.75
***f*-Ir(L_{BM})$_2$(L_{BI})**	0.28	377	–5.08	3.29	–1.79
Ir_2(Js1)(L_{BM})$_4$	0.26, 0.38	398	–5.06	3.12	–1.94
Ir_2(Js2)(L_{BM})$_4$	0.21, 0.34	398	–5.01	3.12	–1.89
Ir_2(Js3)(L_{BM})$_4$	0.26, 0.42	426	–5.06	2.91	–2.15
Ir_2(Js3)(L_{IM})$_4$	0.17, 0.32	429	–4.97	2.89	–2.08

[a] $E^{ox}_{½}$ refers to [(E_{pa} + E_{pc})/2], where E_{pa} and E_{pc} are the anodic and cathodic peak potentials referenced to the Fc/Fc^+ couple (Fc/Fc^+ = 0.38 V) in CH_2Cl_2 solution at RT.

[b] E_{HOMO} = −(E_{ox} + 4.8) eV, E_g = 1240/$\lambda_{PL\ onset}$, and E_{LUMO} = E_{HOMO} + E_g.

Table S2. Crystal data and structure refinement for ***f*-Ir(L_{BM})$_2$(L_{BI})**

CCDC number	2493846
Empirical formula	$C_{77}H_{87}Cl_2IrN_6$
Formula weight	1359.62
Temperature [K]	213(2)
Crystal system	monoclinic
Space group (number)	(14)
a [Å]	13.1678(4)
b [Å]	45.4005(13)
c [Å]	11.9060(3)
α [°]	90
β [°]	107.720(2)
γ [°]	90
Volume [Å^3]	6780.0(3)
Z	4
ρ_{calc} [gcm^{-3}]	1.332
μ [mm^{-1}]	4.891
F(000)	2808
Crystal size [mm^3]	0.03×0.17×0.28
Crystal colour	colourless
Crystal shape	block
Radiation	Cu K_α (λ=1.54178 Å)
2θ range [°]	3.89 to 150.44 (0.80 Å)
Index ranges	$-14 \leq h \leq 16$; $-56 \leq k \leq 55$; $-14 \leq l \leq 14$
Reflections collected	50789
Independent reflections	13747; R_{int} = 0.0844; R_{sigma} = 0.0786
Completeness to θ = 67.679°	99.1
Data / Restraints / Parameters	13747 / 108 / 822
Goodness-of-fit on F^2	1.045
Final *R* indexes [$I \geq 2\sigma(I)$]	R_1 = 0.0488; wR_2 = 0.1243
Final *R* indexes [all data]	R_1 = 0.0632 wR_2 = 0.1338
Largest peak/hole [eÅ^{-3}]	2.00/−0.80

Table S3. Crystal data and structure refinement for $\mathbf{Ir_2(Js1)(L_{BM})_4}$

CCDC number	2493844
Empirical formula	$C_{144}H_{160}Cl_{12}Ir_2N_{12}$
Formula weight	2868.63
Temperature [K]	253(2)
Crystal system	monoclinic
Space group (number)	(15)
a [Å]	24.7568(17)
b [Å]	23.5695(18)
c [Å]	28.5975(19)
α [°]	90
β [°]	108.311(2)
γ [°]	90
Volume [Å^3]	15841.9(19)
Z	4
ρ_{calc} [gcm^{-3}]	1.203
μ [mm^{-1}]	5.424
F(000)	5864
Crystal size [mm^3]	0.04×0.14×0.29
Crystal colour	colourless
Crystal shape	block
Radiation	Cu K_α (λ=1.54178 Å)
2θ range [°]	6.82 to 149.70 (0.80 Å)
Index ranges	$-30 \leq h \leq 30$; $-29 \leq k \leq 29$; $-35 \leq l \leq 33$
Reflections collected	131736
Independent reflections	16248*;* R_{int} = 0.0574*;* R_{sigma} = 0.0343
Completeness to θ = 67.679°	99.9
Data / Restraints / Parameters	16248 / 2335 / 1114
Goodness-of-fit on F^2	1.059
Final *R* indexes [$I \geq 2\sigma(I)$]	R_1 = 0.0318; wR_2 = 0.0881
Final *R* indexes [all data]	R_1 = 0.0348; wR_2 = 0.0902
Largest peak/hole [eÅ^{-3}]	0.64 / −0.98
Extinction coefficient	0.000115(7)

Table S4. Crystal data and structure refinement for $\mathbf{Ir_2(Js2)(L_{BM})_4}$

CCDC number	2493845
Empirical formula	$C_{150}H_{172}Cl_8Ir_2N_{12}$
Formula weight	2810.99
Temperature [K]	213(2)
Crystal system	monoclinic
Space group (number)	(13)
a [Å]	33.7477(18)
b [Å]	12.4772(7)
c [Å]	33.9723(18)
α [°]	90
β [°]	95.452(3)
γ [°]	90
Volume [Å^3]	14240.2(13)
Z	4
ρ_{calc} [gcm^{-3}]	1.311
μ [mm^{-1}]	5.348
F(000)	5784
Crystal size [mm^3]	0.02×0.03×0.35
Crystal colour	colourless
Crystal shape	needle
Radiation	CuK_α (λ=1.54178 Å)
2θ range [°]	3.88 to 149.62 (0.80 Å)
Index ranges	$-36 \leq h \leq 42$; $-13 \leq k \leq 15$; $-42 \leq l \leq 41$
Reflections collected	105777
Independent reflections	28872; R_{int} = 0.1205; R_{sigma} = 0.1182
Completeness to θ = 67.679°	99.0
Data / Restraints / Parameters	28872 / 1160 / 1786
Goodness-of-fit on F^2	1.070
Final *R* indexes [$I \geq 2\sigma(I)$]	R_1 = 0.0692; wR_2 = 0.1755
Final *R* indexes [all data]	R_1 = 0.1028; wR_2 = 0.1951
Largest peak/hole [eÅ^{-3}]	2.28/−2.07

Table S5. Crystal data and structure refinement for **Ir_2(Js3)(L_{IM})$_4$**

CCDC number	2493847
Empirical formula	$C_{131.50}H_{144}ClIr_2N_{13}$
Formula weight	2326.44
Temperature [K]	193(2)
Crystal system	orthorhombic
Space group (number)	(37)
a [Å]	39.8974(9)
b [Å]	14.5469(3)
c [Å]	22.9823(5)
α [°]	90
β [°]	90
γ [°]	90
Volume [Å^3]	13338.5(5)
Z	4
ρ_{calc} [gcm^{-3}]	1.158
μ [mm^{-1}]	4.354
F(000)	4780
Crystal size [mm^3]	0.02×0.09×0.28
Crystal colour	yellow
Crystal shape	block
Radiation	Cu K_α (λ=1.54178 Å)
2θ range [°]	6.47 to 149.67 (0.80 Å)
Index ranges	$-49 \leq h \leq 49$; $-18 \leq k \leq 18$; $-28 \leq l \leq 27$
Reflections collected	109555
Independent reflections	13498; R_{int} = 0.0541; R_{sigma} = 0.0308
Completeness to θ = 67.679°	99.9
Data / Restraints / Parameters	13498 / 1634 / 1038
Goodness-of-fit on F^2	1.087
Final *R* indexes [$I \geq 2\sigma(I)$]	R_1 = 0.0260; wR_2 = 0.0652
Final *R* indexes [all data]	R_1 = 0.0275; wR_2 = 0.0661
Largest peak/hole [eÅ^{-3}]	0.72/−0.29
Flack X parameter	0.226(8)

Refinement details for Ir_2(Js3)(L_{IM})$_4$

Refined as a 2-component inversion twin.

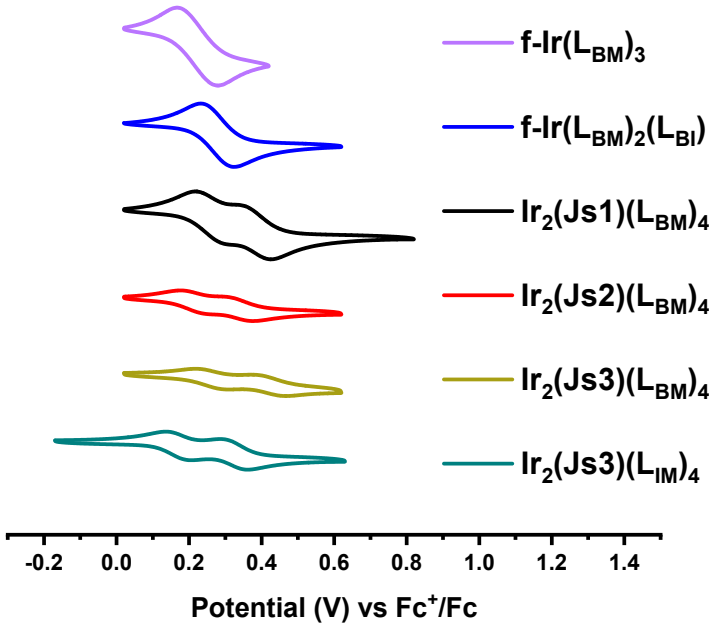

Figure S1. Cyclic voltammograms of all studied Ir(III) complexes in CH_2Cl_2 solution at RT.

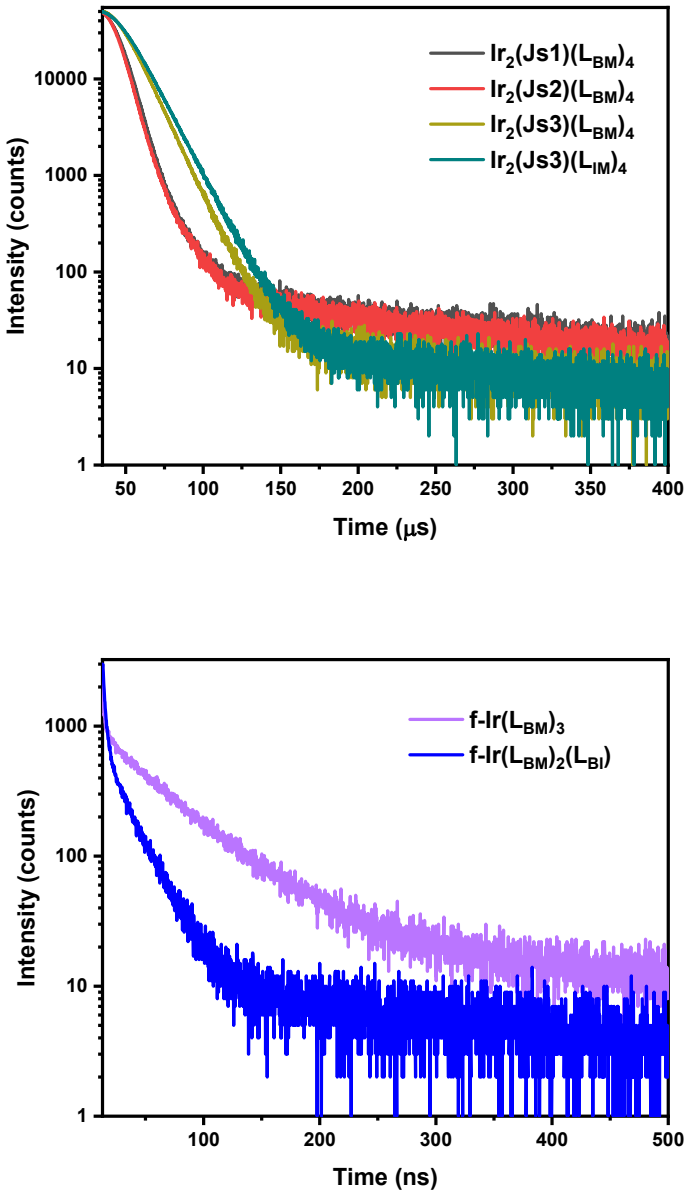

Figure S2. (a) Transient decay of dinuclear Ir(III) complexes with λ_{exc} @ 375 nm and (b) transient decay of mononuclear Ir(III) complexes with λ_{exc} @ 293 nm in degassed toluene at RT.

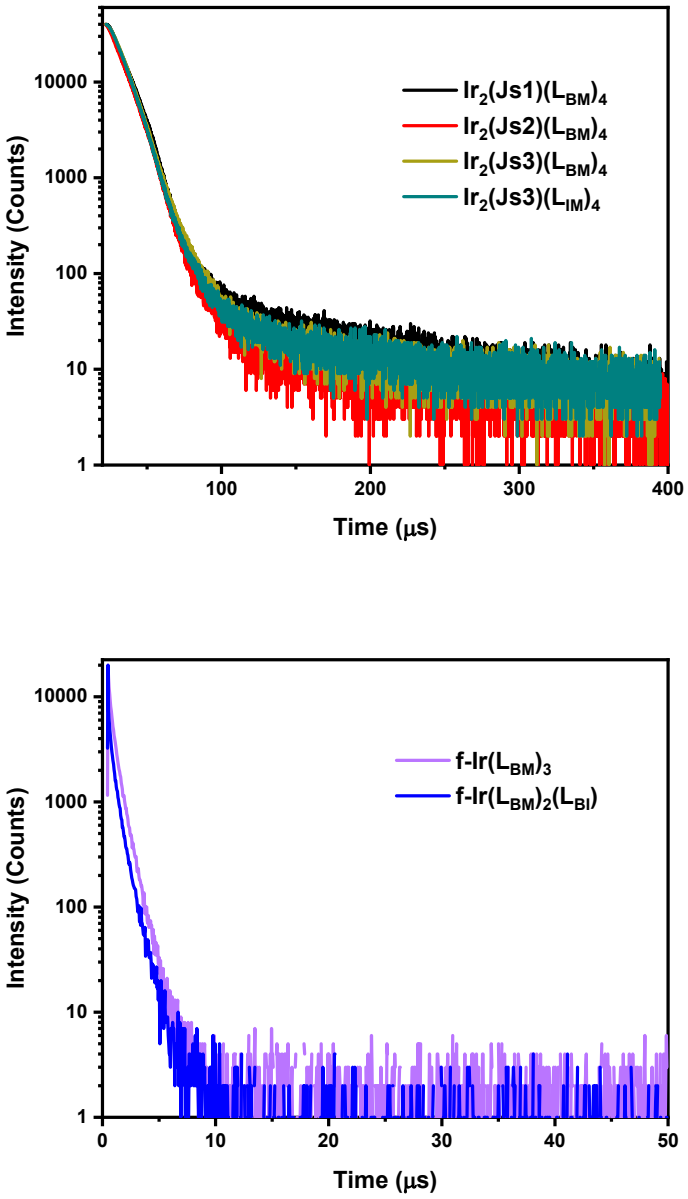

Figure S3. (a) Transient decay of dinuclear Ir(III) complexes with λ_{exc} @ 375 nm and (b) transient decay of mononuclear Ir(III) complexes with λ_{exc} @ 293 nm in drop-cast PS thin film at 2 wt% at RT.

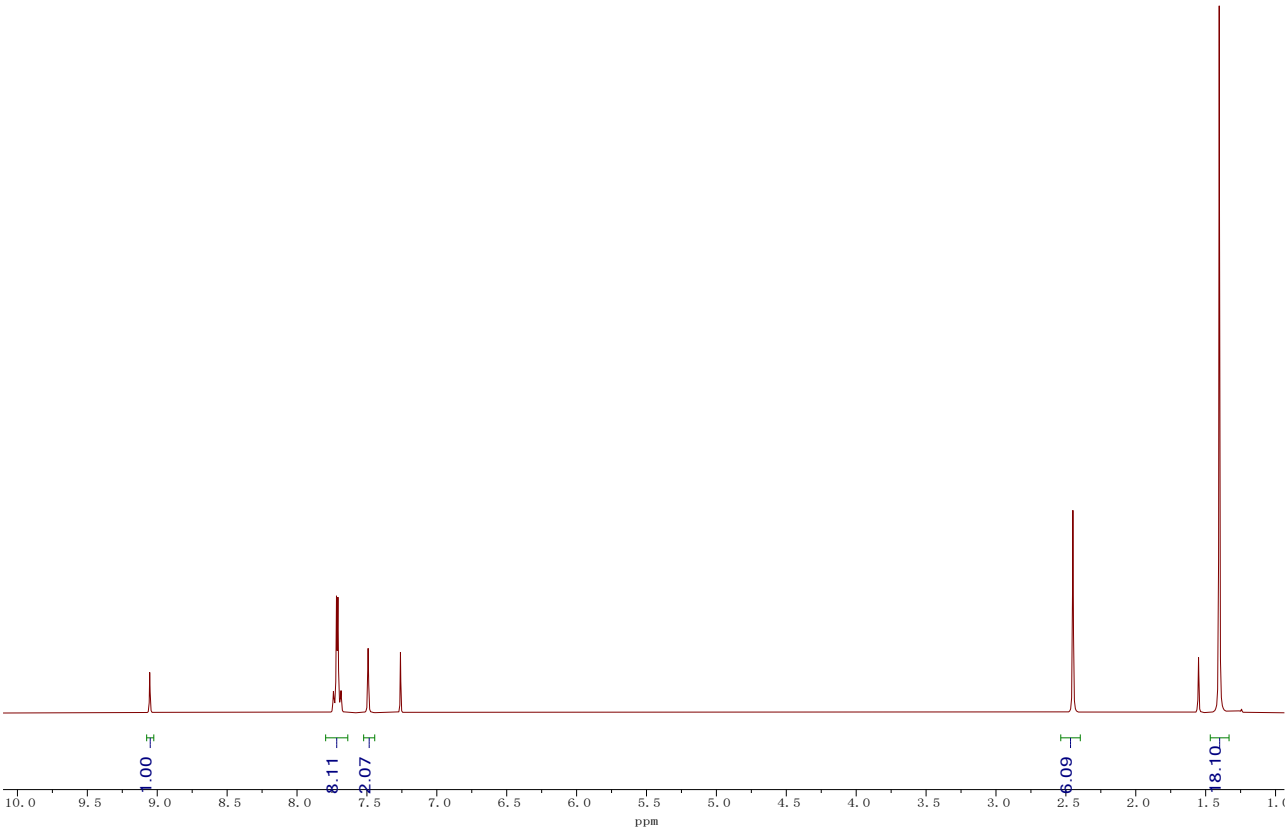

Figure S4. ^{1}H NMR (400 MHz) spectrum of **($L_{BM}H_2$)·PF_6** recorded in $CDCl_3$ at RT.

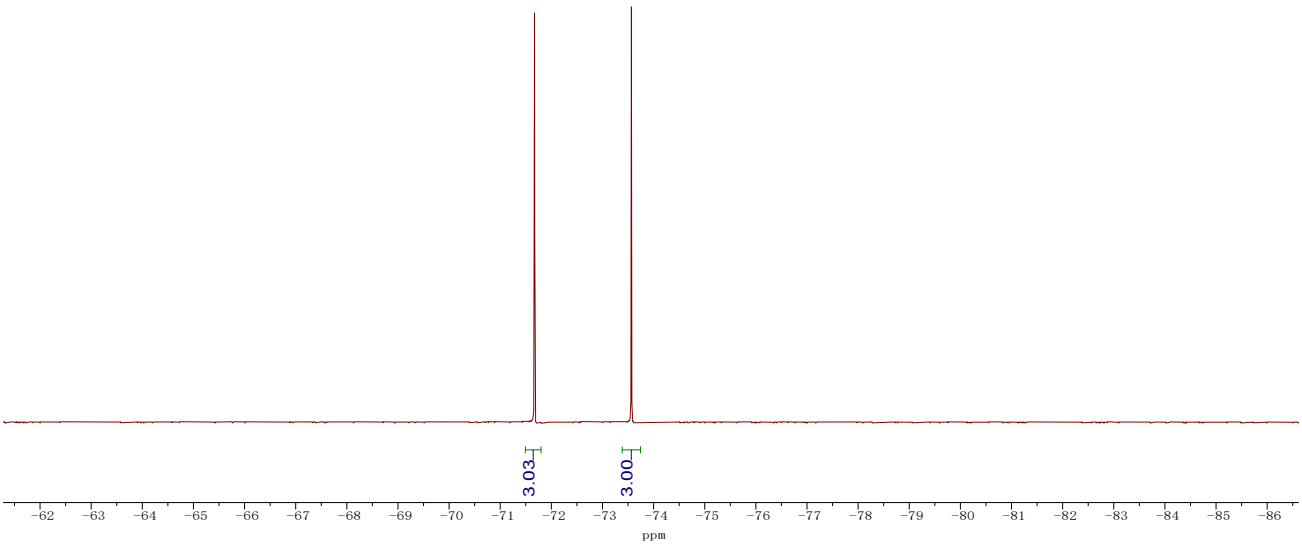

Figure S5. ^{19}F NMR (376 MHz) spectrum of **($L_{BM}H_2$)·PF_6** recorded in $CDCl_3$ at RT.

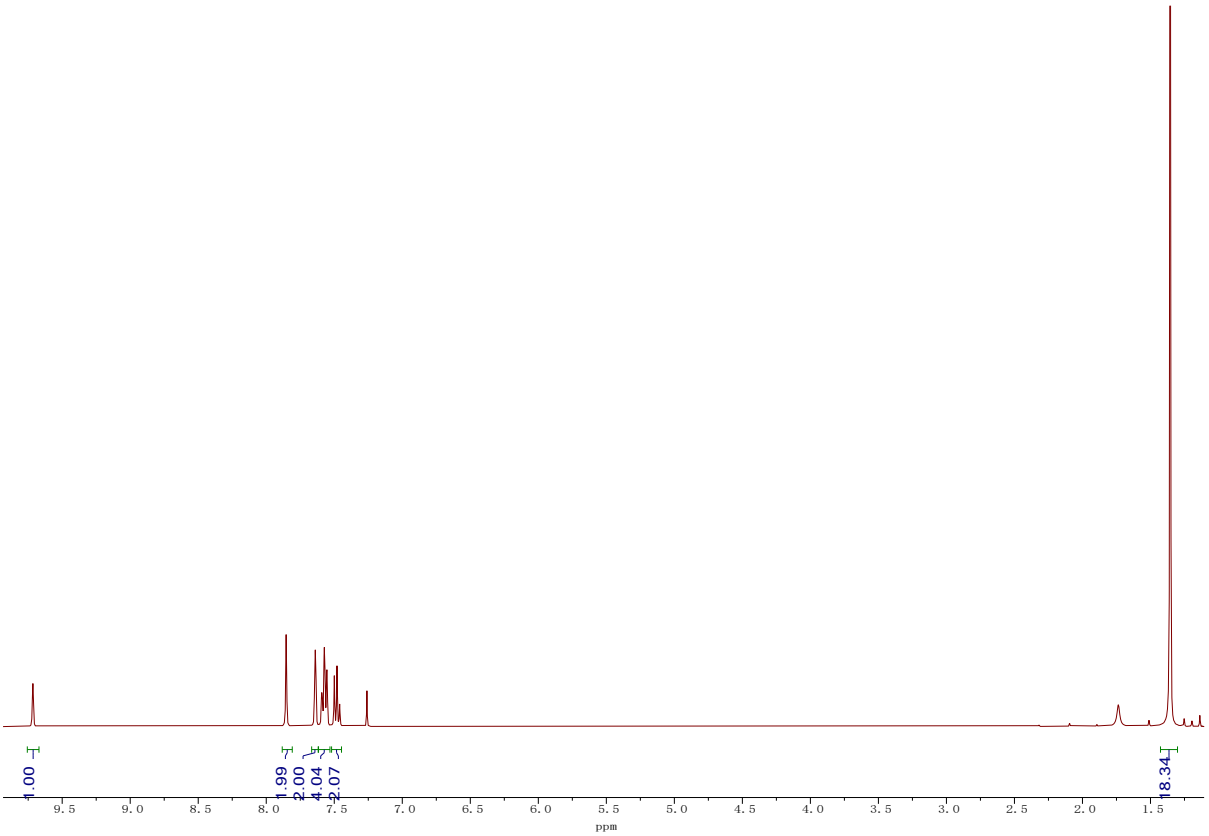

Figure S6. ^{1}H NMR (400 MHz) spectrum of **($L_{IM}H_2$)·OTf** recorded in $CDCl_3$ at RT.

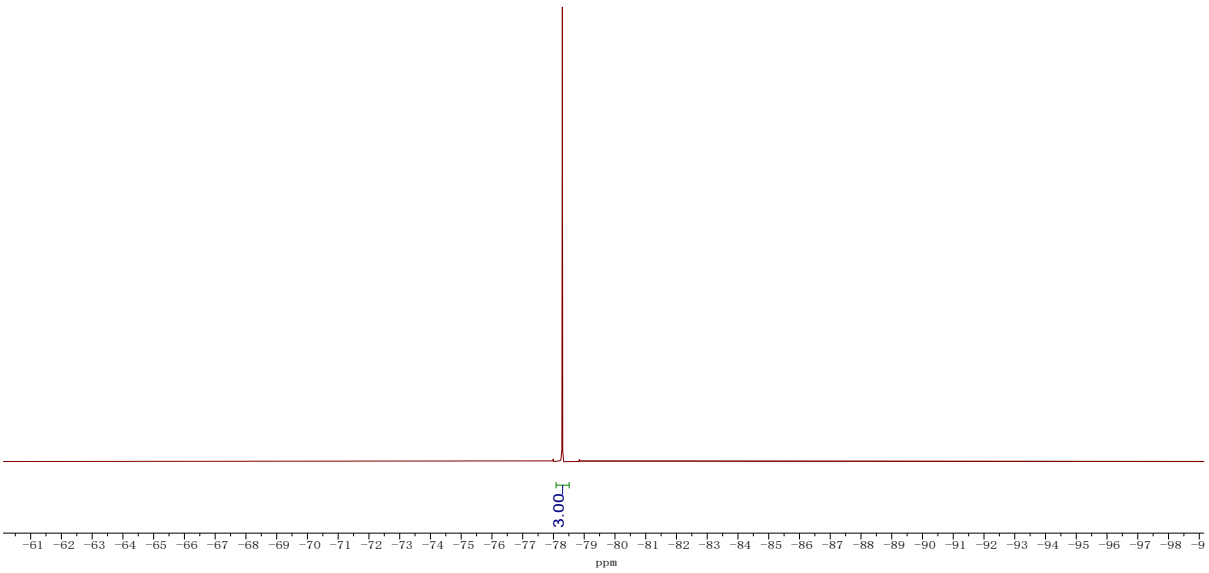

Figure S7. ^{19}F NMR (376 MHz) spectrum of **($L_{IM}H_2$)·OTf** recorded in $CDCl_3$ at RT.

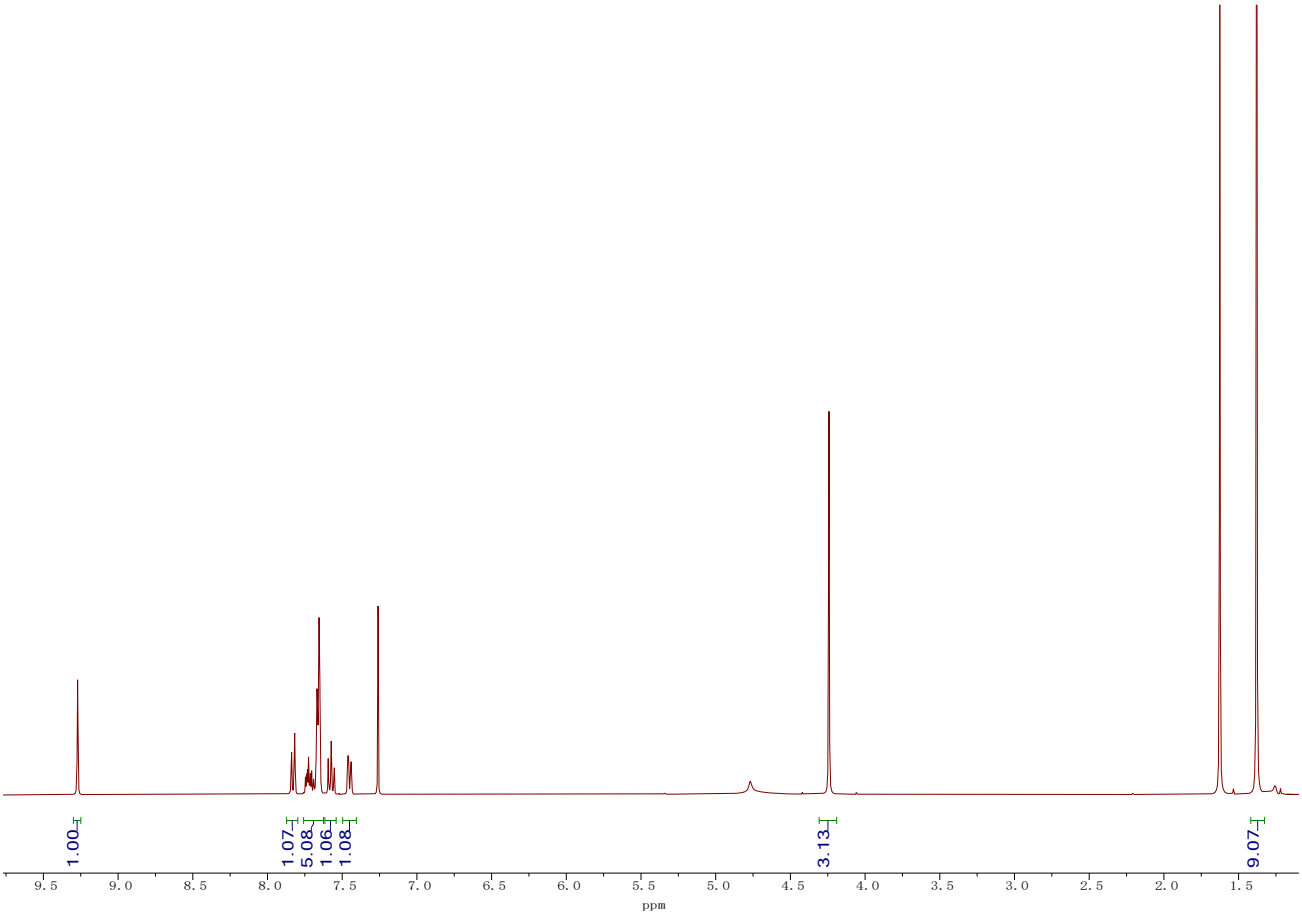

Figure S8. ^{1}H NMR (400 MHz) spectrum of **$(L_{BI}H_2)\cdot PF_6$** recorded in $CDCl_3$ at RT.

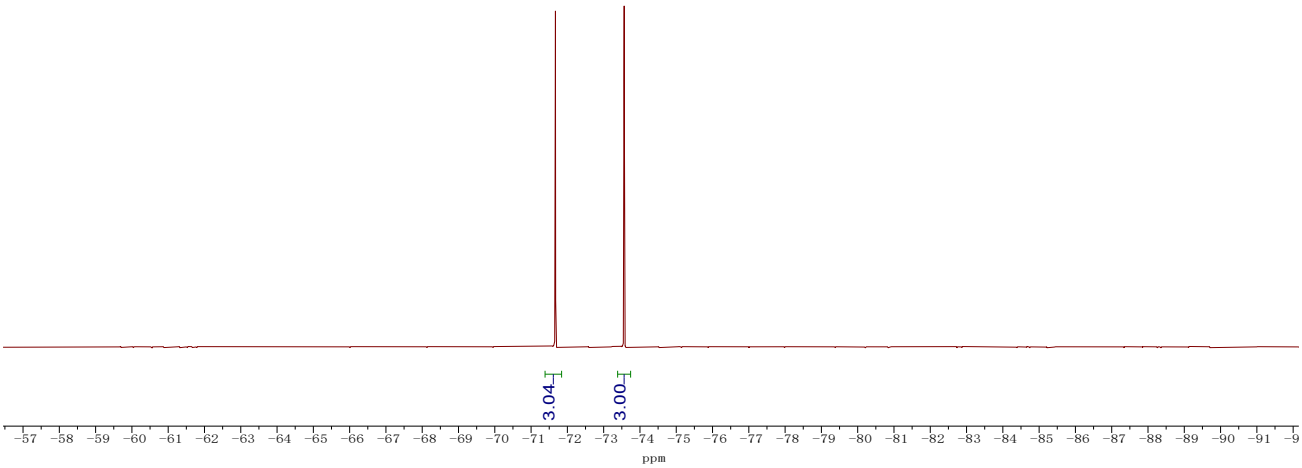

Figure S9. ^{19}F NMR (376 MHz) spectrum of **$(L_{BI}H_2)\cdot PF_6$** recorded in $CDCl_3$ at RT.

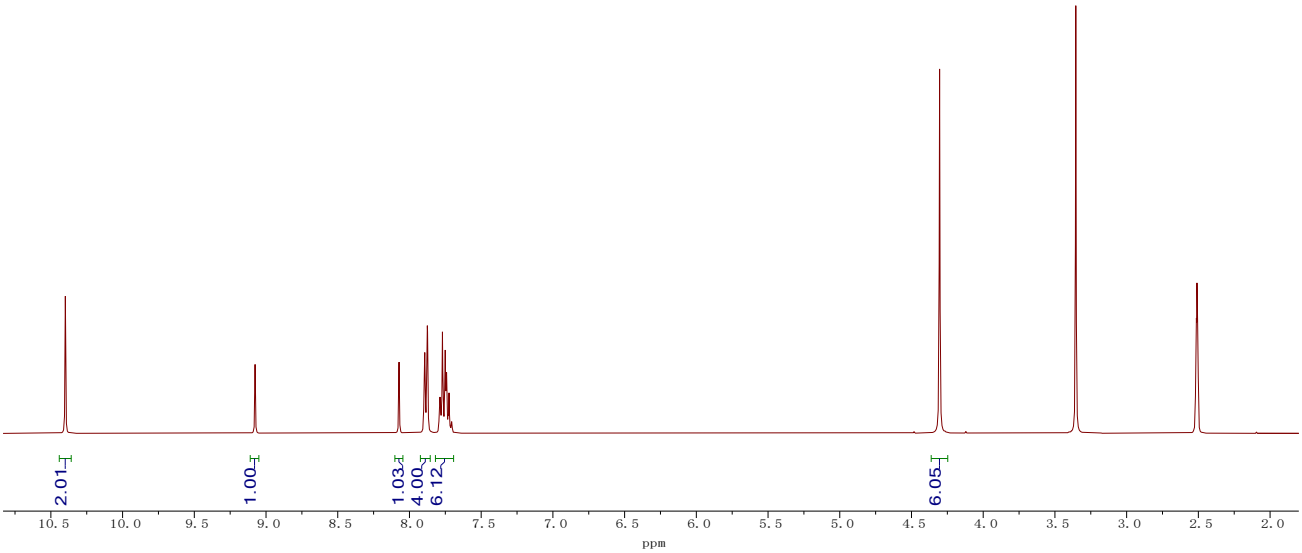

Figure S10. ^{1}H NMR (400 MHz) spectrum of **(Js1H$_4$)·2PF$_6$** recorded in DMSO-d$_6$ at RT.

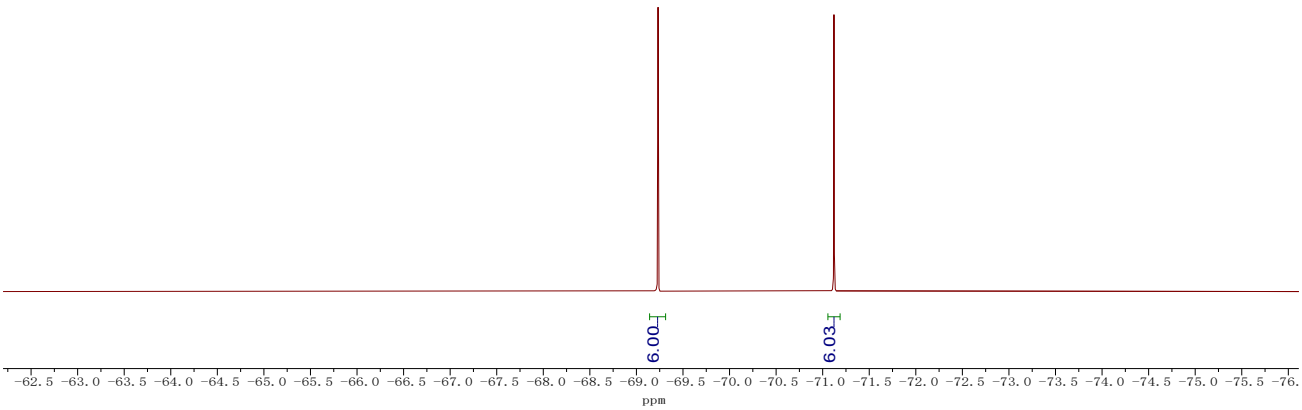

Figure S11. ^{19}F NMR (376 MHz) spectrum of **(Js1H$_4$)·2PF$_6$** recorded in DMSO-d$_6$ at RT.

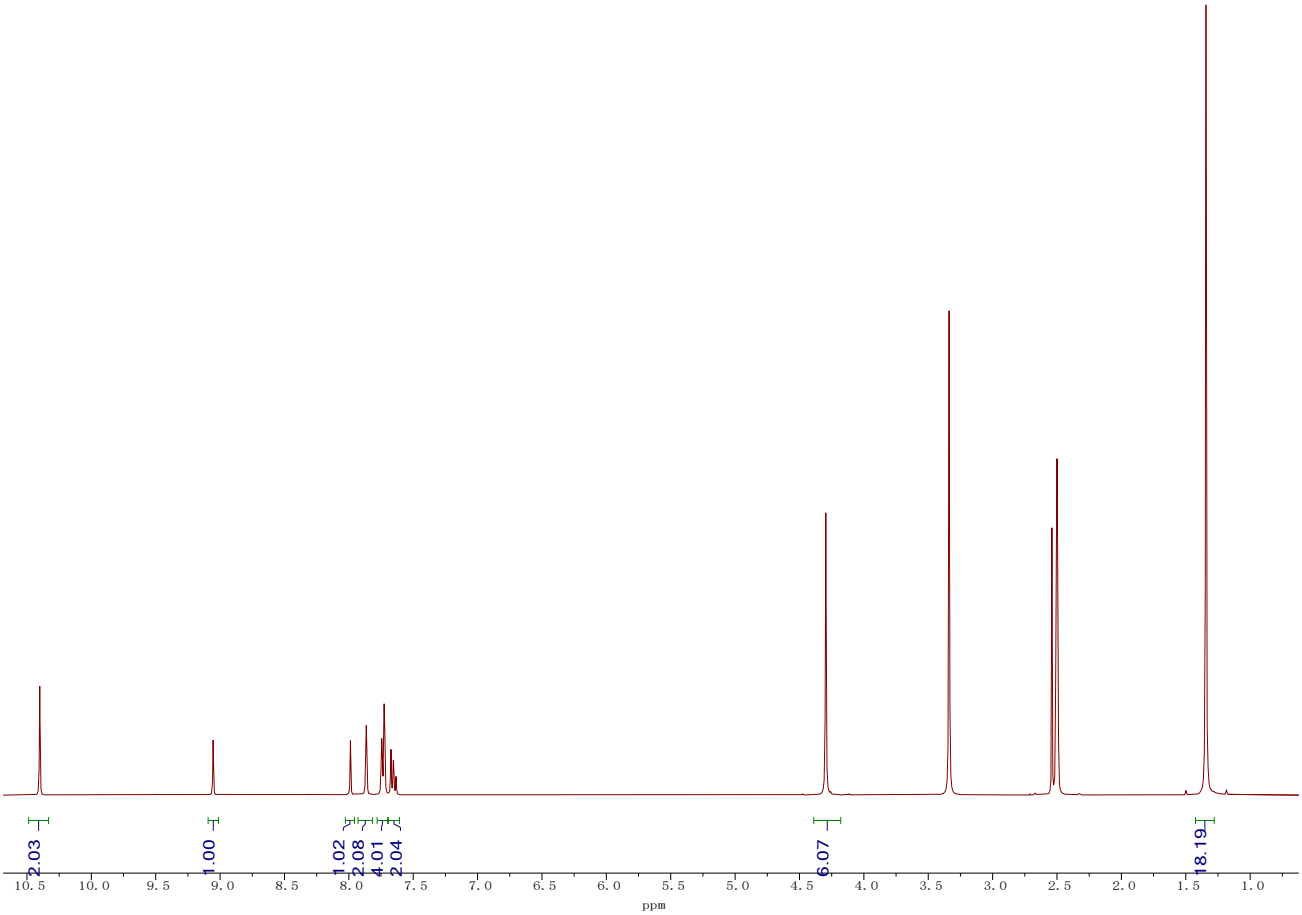

Figure S12. ^{1}H NMR (400 MHz) spectrum of **(Js2H$_4$)·2PF$_6$** recorded in DMSO-d$_6$ at RT.

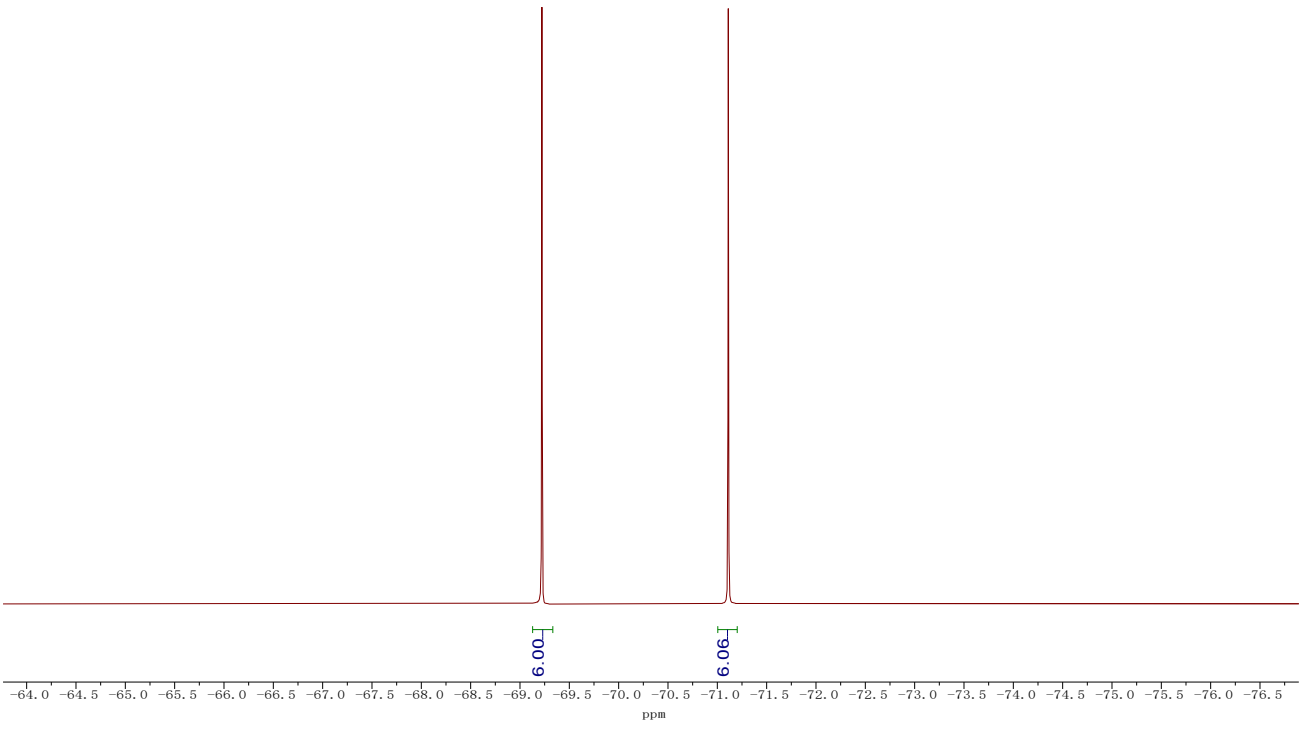

Figure S13. ^{19}F NMR (376 MHz) spectrum of **(Js2H$_4$)·2PF$_6$** recorded in DMSO-d$_6$ at RT.

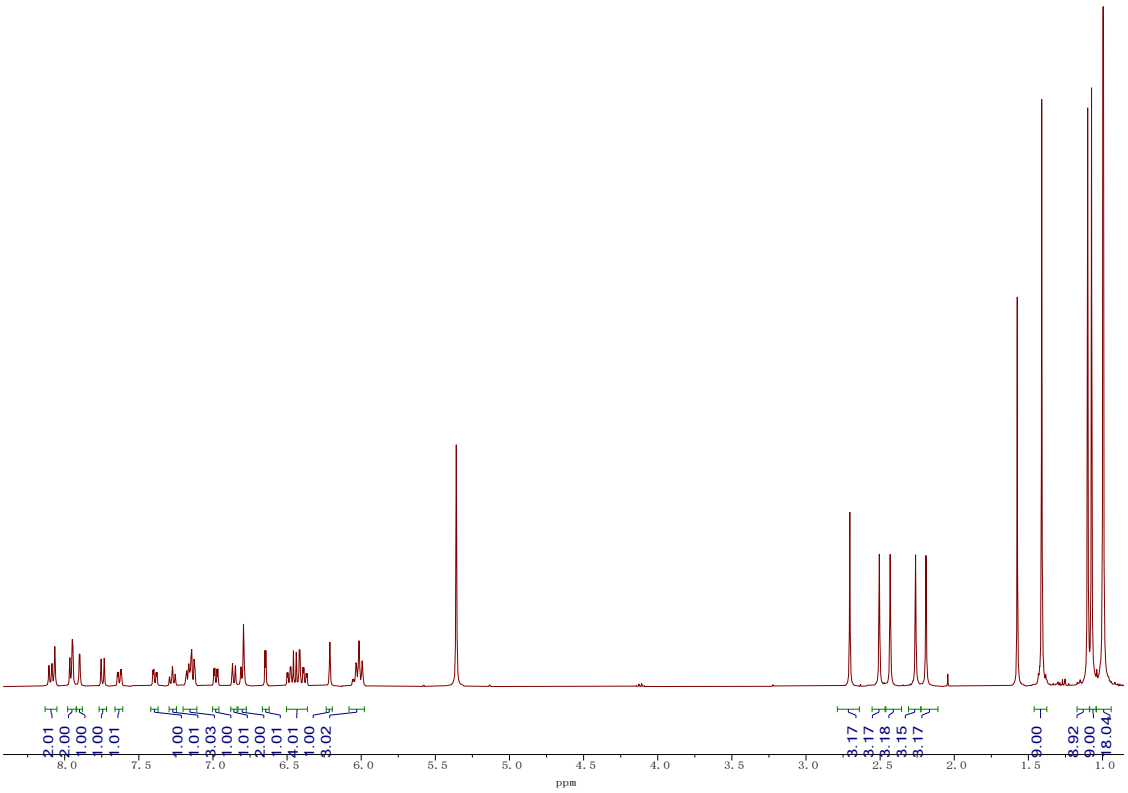

Figure S14. ^{1}H NMR (400 MHz) spectrum of ***f*-Ir(L_{BM})$_2$(L_{BI})** recorded in CD_2Cl_2 at RT.

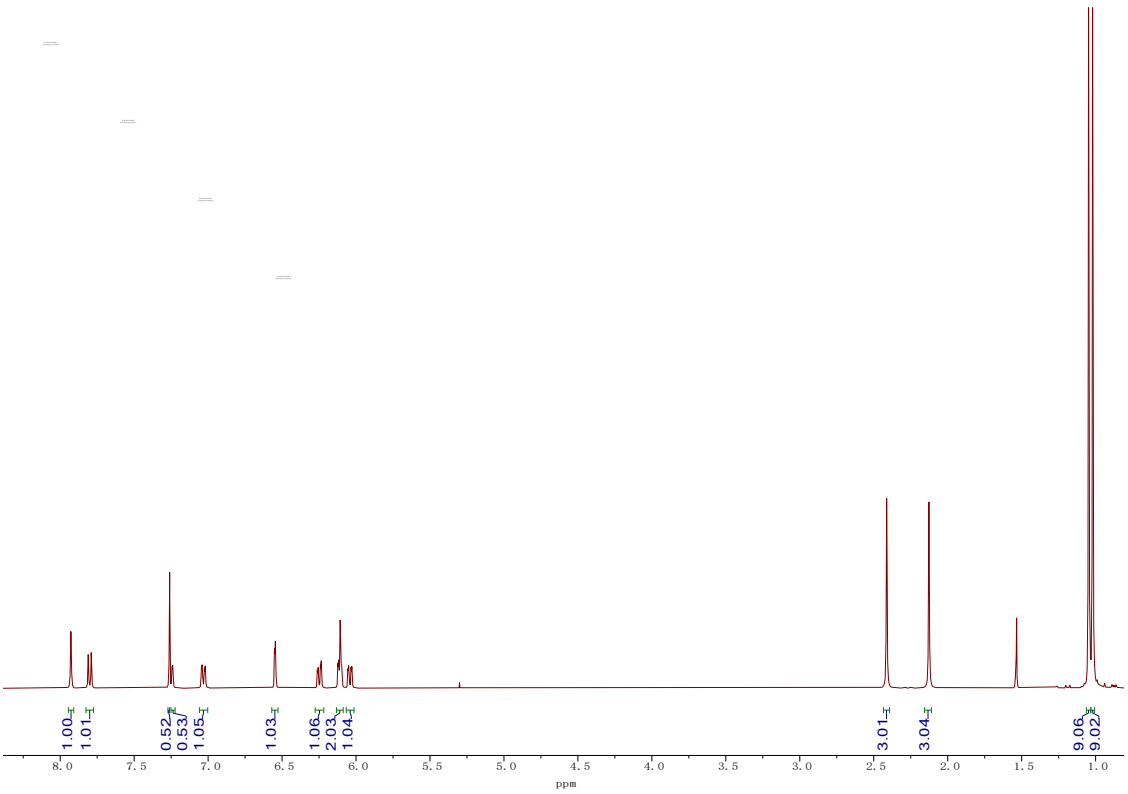

Figure S15. ^{1}H NMR (400 MHz) spectrum of ***f*-Ir(L_{BM})$_3$** recorded in $CDCl_3$ at RT.

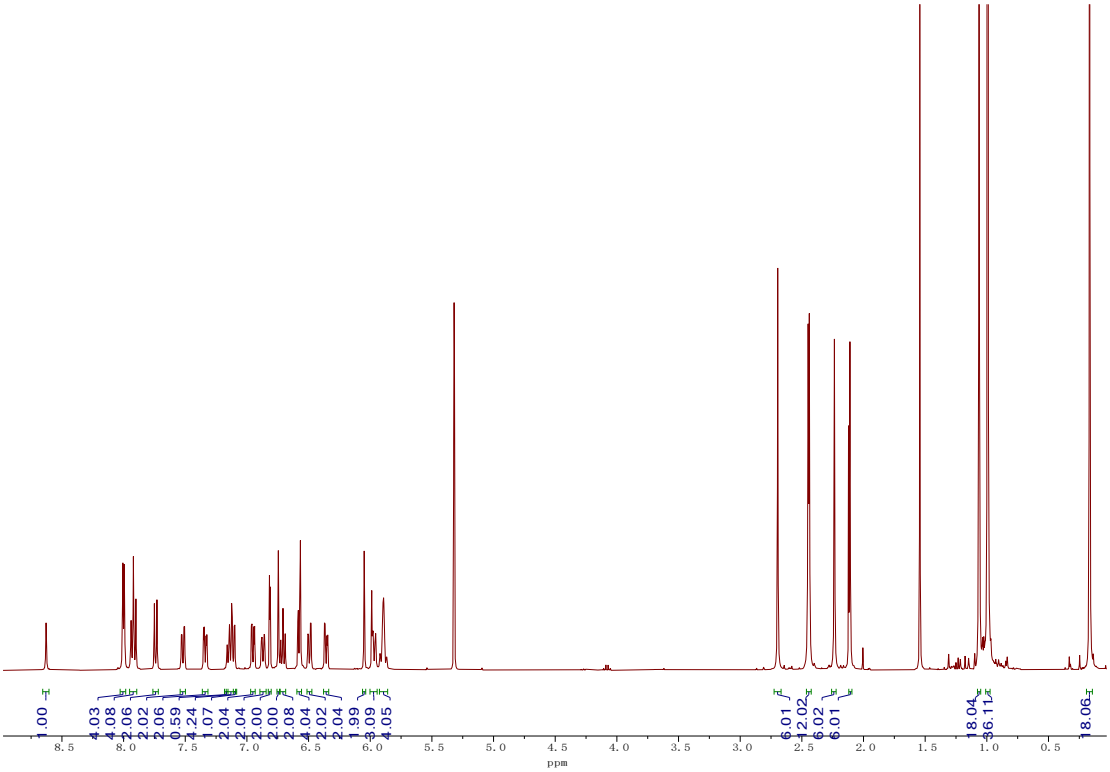

Figure S16. ^{1}H NMR (400 MHz) spectrum of **Ir_2(Js1)(L_{BM})$_4$** recorded in CD_2Cl_2 at RT.

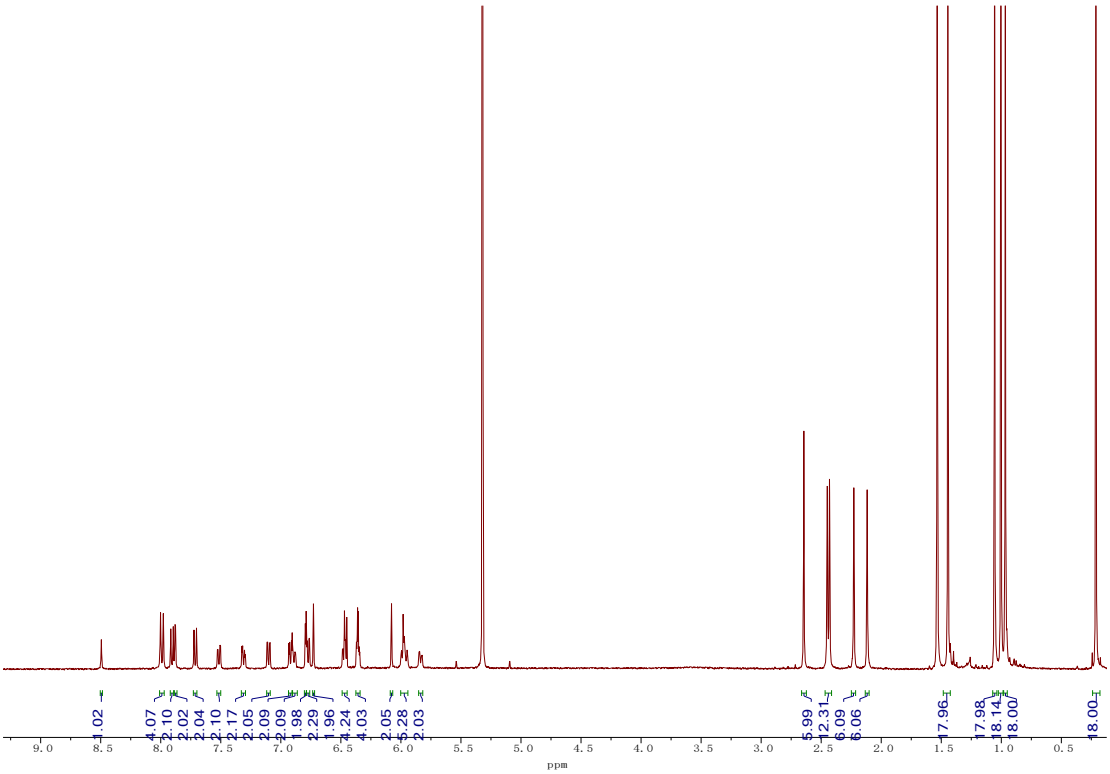

Figure S17. ^{1}H NMR (400 MHz) spectrum of **Ir_2(Js2)(L_{BM})$_4$** recorded in CD_2Cl_2 at RT.

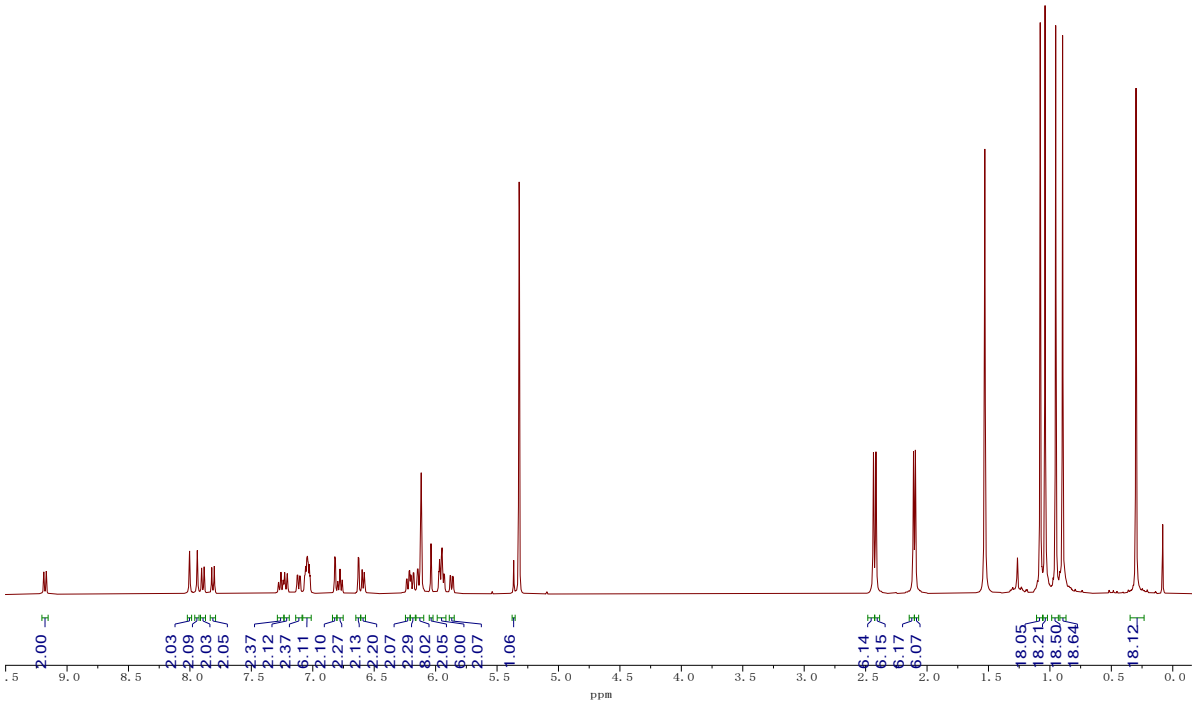

Figure S18. ^{1}H NMR (400 MHz) spectrum of **Ir_2(Js3)(L_{BM})$_4$** recorded in CD_2Cl_2 at RT.

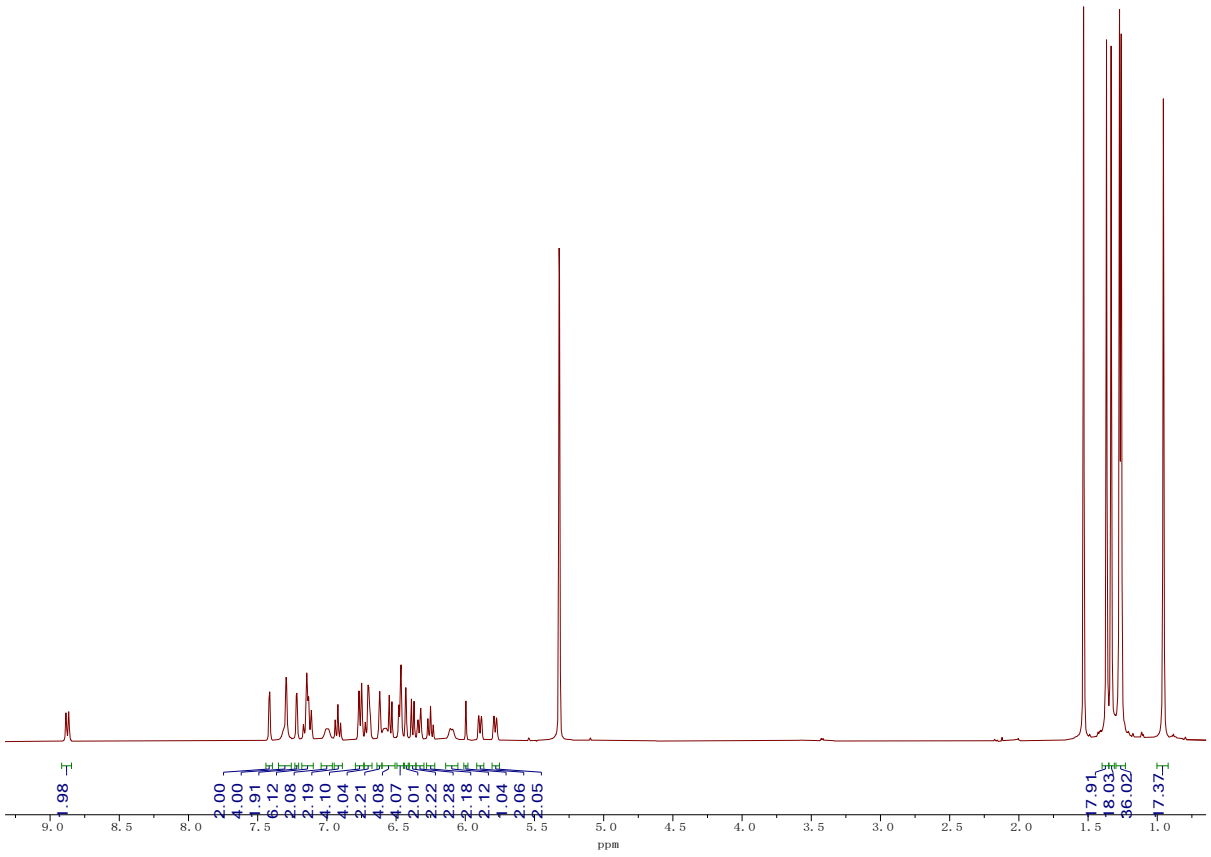

Figure S19. ^{1}H NMR (400 MHz) spectrum of **Ir_2(Js3)(L_{IM})$_4$** recorded in CD_2Cl_2 at RT.

References

1. C. Lee, W. Yang and R. G. Parr, Development of the Colle-Salvetti correlation-energy formula into a functional of the electron density, *Phys. Rev. B*, 1988, **37**, 785-789.
2. A. D. Becke, Density-functional thermochemistry. III. The role of exact exchange, *J. Chem. Phys.*, 1993, **98**, 5648-5652.
3. F. Weigend and R. Ahlrichs, Balanced basis sets of split valence, triple zeta valence and quadruple zeta valence quality for H to Rn: Design and assessment of accuracy, *Phys. Chem. Chem. Phys.*, 2005, **7**, 3297-3305.
4. F. Weigend, Accurate Coulomb-fitting basis sets for H to Rn, *Phys. Chem. Chem. Phys.*, 2006, **8**, 1057-1065.
5. S. Grimme, S. Ehrlich and L. Goerigk, Effect of the damping function in dispersion corrected density functional theory, *J. Comput. Chem.*, 2011, **32**, 1456-1465.
6. M. J. Frisch, G. W. Trucks, H. B. Schlegel, G. E. Scuseria, M. A. Robb, J. R. Cheeseman, G. Scalmani, V. Barone, B. Mennucci, G. A. Petersson, H. Nakatsuji, M. Caricato, X. Li, H. P. Hratchian, A. F. Izmaylov, J. Bloino, G. Zheng, J. L. Sonnenberg, M. Hada, M. Ehara, K. Toyota, R. Fukuda, J. Hasegawa, M. Ishida, T. Nakajima, Y. Honda, O. Kitao, H. Nakai, T. Vreven, J. A. Montgomery, J. E. Peralta, F. Ogliaro, M. Bearpark, J. J. Heyd, E. Brothers, K. N. Kudin, V. N. Staroverov, R. Kobayashi, J. Normand, K. Raghavachari, A. Rendell, J. C. Burant, S. S. Iyengar, J. Tomasi, M. Cossi, N. Rega, J. M. Millam, M. Klene, J. E. Knox, J. B. Cross, V. Bakken, C. Adamo, J. Jaramillo, R. Gomperts, R. E. Stratmann, O. Yazyev, A. J. Austin, R. Cammi, C. Pomelli, J. W. Ochterski, R. L. Martin, K. Morokuma, V. G. Zakrzewski, G. A. Voth, P. Salvador, J. J. Dannenberg, S. Dapprich, A. D. Daniels, Ö. Farkas, J. B. Foresman, J. V. Ortiz, J. Cioslowski and D. J. Fox, Gaussian 16, Revision C.01, *Gaussian 16, Revision C.01; Gaussian Inc.*, 2016, Wallingford, CT.
7. S. Miertuš, E. Scrocco and J. Tomasi, Electrostatic interaction of a solute with a continuum. A direct utilizaion of AB initio molecular potentials for the prevision of solvent effects, *Chem. Phys.*, 1981, **55**, 117-129.
8. S. Miertuš and J. Tomasi, Approximate evaluations of the electrostatic free energy and internal energy changes in solution processes, *Chem. Phys.*, 1982, **65**, 239-245.
9. C. Adamo and D. Jacquemin, The calculations of excited-state properties with Time-Dependent Density Functional Theory, *Chem. Soc. Rev.*, 2013, **42**, 845-856.
10. A. D. Laurent, C. Adamo and D. Jacquemin, Dye chemistry with time-dependent density functional theory, *Phys. Chem. Chem. Phys.*, 2014, **16**, 14334-14356.
11. R. L. Martin, Natural Transition Orbitals, *J. Chem. Phys.*, 2003, **118**, 4775-4777.
12. T. Lu and F. Chen, Multiwfn: A multifunctional wavefunction analyzer, *J. Comput. Chem.*, 2012, **33**, 580-592.
13. F. L. Hirshfeld, Bonded-atom fragments for describing molecular charge densities, *Theo. Chim. Acta*, 1977, **44**, 129-138.
14. B. de Souza, G. Farias, F. Neese and R. Izsák, Predicting Phosphorescence Rates of Light Organic Molecules Using Time-Dependent Density Functional Theory and the Path Integral Approach to Dynamics, *J. Chem. Theory Comput.*, 2019, **15**, 1896-1904.
15. E. van Lenthe, E. J. Baerends and J. G. Snijders, Relativistic regular two-component

Hamiltonians, *J. Chem. Phys.*, 1993, **99**, 4597-4610.
16. E. van Lenthe, E. J. Baerends and J. G. Snijders, Relativistic total energy using regular approximations, *J. Chem. Phys.*, 1994, **101**, 9783-9792.
17. F. Neese, F. Wennmohs, U. Becker and C. Riplinger, The ORCA quantum chemistry program package, *J. Chem. Phys.*, 2020, **152**, 224108.
18. C. C. Pye and T. Ziegler, An implementation of the conductor-like screening model of solvation within the Amsterdam density functional package, *Theor. Chem. Acc.*, 1999, **101**, 396-408.